

REPORT DOCUMENTATION PAGE			Form Approved OMB No. 0704-0188	
Public reporting burden for this collection of information is estimated to average 1 hour per response, including the time for reviewing instructions, searching existing data sources, gathering and maintaining the data needed, and completing and reviewing the collection of information. Send comments regarding this burden estimate or any other aspect of this collection of information, including suggestions for reducing this burden, to Washington Headquarters Services, Directorate for Information Operations and Reports, 1. 15 Jefferson Davis Highway, Suite 1204, Arlington, VA 22202-4302, and to the Office of Management and Budget, Paperwork Reduction Project (0704-0188), Washington, DC 20503.				
1. AGENCY USE ONLY (Leave blank)		2. REPORT DATE 03/07/96	3. REPORT TYPE AND DATES COVERED Final Technical Mar 93 - 29 Feb 96	
4. TITLE AND SUBTITLE Development of Multifunctional Polymers			5. FUNDING NUMBERS F49620-93-1-0195	
6. AUTHOR(S) Luping Yu			61102F 2303/CS	
7. PERFORMING ORGANIZATION NAME(S) AND ADDRESS(ES) The University of Chicago Department of Chemistry 5735 S. Ellis Avenue Chicago, IL 60637			8. PERFORMING ORGANIZATION REPORT NUMBER AFOSR-TR-96 0150	
9. SPONSORING/MONITORING AGENCY NAME(S) AND ADDRESS(ES) AFOSR/NL 110 Duncan Avenue Bolling AFB DC 20332-8080 Dr Charles Y-C Lee				
11. SUPPLEMENTARY NOTES				
12a. DISTRIBUTION/AVAILABILITY STATEMENT Reproduction in whole or in part is permitted for any of the United States Government. This document has been approved for public release and sale; its distribution is unlimited			12b. DISTRIBUTION CODE	
13. ABSTRACT (Maximum 200 words) This final report summarizes research works on photorefractive materials which are single chain, fully functionalized polymers. Three polymeric systems were described, namely, functionalized polyurethanes, functionalized conjugated polymers and polyimides containing porphyrin moieties. Detailed synthetic procedures were outlined. Extensive physical studies, including photoconductivity measurements, electro-optic measurements and two beam coupling studies were carried out. The results revealed the unique features for fully functional, photorefractive polymers. This work also lead to the development of a novel synthetic methodology for polycondensation by utilizing the Stille coupling reaction.				
14. SUBJECT TERMS			15. NUMBER OF PAGES	
			16. PRICE CODE	
17. SECURITY CLASSIFICATION OF REPORT None			18. SECURITY CLASSIFICATION OF THIS PAGE None	
19. SECURITY CLASSIFICATION OF ABSTRACT None			20. LIMITATION OF ABSTRACT Unlimited	

19960404 058

# **Final Technical Report**

**Report Period: 03/01/93-02/29/96**

**Air Force Office of Scientific Research**

**Grant Number: F49620-93-1-0195**

**"Development of Multifunctional Polymers"**

**Prepared by**

**Professor Luping Yu**

**Department of Chemistry and James Frank Institute,**

**The University of Chicago, 5735 S. Ellis Avenue,**

**Chicago, IL-60637**

## Papers Published Under Sponsorship of AFOSR Grant (F49620-93-1-0195)

1. L. P. Yu, W. K. Chan, Z. N. Bao and Simon Cao, "Photorefractive Polymer 2-Structural Design and Property Characterization", *Macromolecules.*, 26, 2216, (1993).
2. L. P. Yu, W. K. Chan, Y. M. Chen, , Z. H. Peng and Z. N. Bao, *Polymer Preprints*, 34 (2), 536 (1993).
3. L. P. Yu, W. K. Chan, Y. M. Chen, Z. H. Peng and Z. N. Bao, "Rational Designs of multifunctional Polymers", *Polymer Preprints*, 34 (2), 536, (1993).
4. Y. M. Chen, W. K. Chan, Z. H. Peng, D. Yu and L. P. Yu, "A Novel Polymeric Material for Photorefractive Applications" *Polymer Preprints*, 34 (2), 430, (1993).
5. W. K. Chan, Y. M. Chen, Z. H. Peng and L. P. Yu, "Rational Designs of Multifunctional Polymers", *J. Am. Chem. Soc.*, 115, 11735, (1993).
6. L. P. Yu, W. K. Chan, Y. M. Chen, Z. H. Peng, Z. N. Bao and D. Yu, "Novel Photorefractive Polymers-Structure Design and Property Characterization", *Proc.SPIE -Int. Soc. Opt. Eng.*, 2025, 268, (1993).
7. Y. M. Chen, Z. H. Peng, W. K. Chan and L. P. Yu, "A New Photorefractive Polymer Based on Multifunctional Polyurethane", *Appl. Phys. Lett*, 64, 1195, (1994).
8. L. P. Yu, Y. M. Chen, W. K. Chan and Z. H. Peng, "Conjugated Photorefractive Polymers", *Appl. Phys. Lett.* 64, 2489, (1994).
9. Z. H. Peng, Z. N. Bao, Y. M. Chen and L. P. Yu, "Large Photorefractivity in an Exceptionally Thermo-Stable Multifunctional Polyimide". *J. Am. Chem. Soc.* 116, 6003, (1994).
10. L. P. Yu, W. K. Chan, Y. M. Chen, and Z. H. Peng; "Rational Designs of Multifunctional Polymers-Conjugated Photorefractive Polymers", *Mat. Res. Soc. Proc. Symp. Proc.*, eds., A. Garito, A. Jen, L. Dalton and C. Lee, Vol. 328, 63, (1994).
11. L. P. Yu and Z. H. Peng, "Design, Synthesis and Characterization of Multifunctional Polyimides for Photonics", *Polym. Mater.:Sci. and Eng.*, 71, 441, (1994).
12. W. K. Chan and L. P. Yu, "Design and Synthesis of Novel Conjugated Photorefractive Polymers", *Polymer Preprint*, 35, 98, (1994).
13. L. P. Yu, Y. M. Chen, and W. K. Chan, "Detailed Studies on A New Conjugated Photorefractive Polymer", *J. Phys. Chem.*, 99, 2797, (1995).
14. L. P. Yu, W. K. Chan and A. Gharavi, *Polym. Mater. Sci and Eng.*, 72, 219, (1995).
15. Z. N. Bao and L. P. Yu, "Polymers Containing Metalloporphyrins, Synthesis, Characterization and Physical Properties", *Trends in Polymer Science.*, 3, 159, (1995).
16. W. K. Chan, and L. P., Yu, "Studies of Functionalized Poly(Phenylenevinylene)s", *Macromolecules*, 28, 6410, (1995)..

17. Z. N. Bao, W. K. Chan and L. P. Yu, "Exploration of the Stille Coupling Reaction for the Synthesis of Functional Polymers", *J. Am. Chem. Soc.*, 117, 12426, (1995).
18. L. P. Yu, W. K. Chan, Z. H. Peng and A. R. Gharavi, "Multifunctional Polymers Exhibiting Photorefractive Effects", *Account of Chemical Research*, 29, 13, (1996).
19. L. P. Yu, W. K. Chan, Z. H. Peng, W. J. Li and A. R. Gharavi, "Photorefractive Polymers", Invited Book chapter in "*Organic Conductive Molecules and Polymers*", Ed. H. S. Nalwa. John Wiley and Sons, New York, To appear in 1996.

## Introduction

Photorefractive (PR) materials are multifunctional materials which combine photoconductivity and an electro-optic (E-O) response to manifest a photorefractive effect.<sup>1</sup> In these materials, the indices of refraction can be modulated by a light via their E-O effect (Pockel effect) and a photoinduced space charge field. It is believed that there are four basic processes involved in the photorefractive effect: the photogeneration of charge carriers upon absorbing photons, the transport of the generated charge carriers either by thermal diffusion or electric drifting, the trap of the charge carriers in the trapping centers which results in the charge separation and the formation of the space charge field, and the formation of a phase grating due to the space charge field modulation of the refractive index via the linear electro-optical effect.<sup>1</sup> Figure 1 illustrates these basic processes.

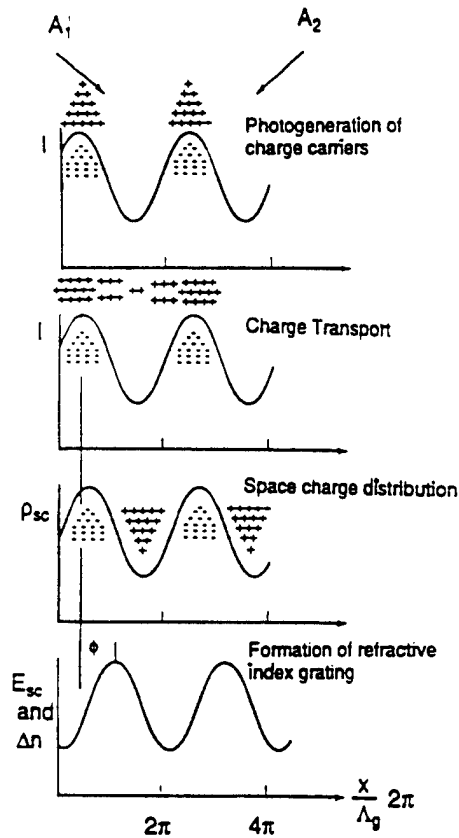


**Figure 1.** Schematic view of the processes involved in the photorefractive effect. Two laser beams were applied.

Notice that two light beams are needed to generate the oscillating space charge field. A unique feature of the space charge field is that it has a phase shift from the interference pattern. This feature results in a special property for photorefractive materials: the optical energy of the two incident beams can exchange in an asymmetric way; one of the beams will lose energy and the other beam will gain energy.

The driving force behind the study of photorefractive materials is their potential application, such as in three-dimensional holographic light processing, phase conjugation and the handling of large quantities of information in real time.<sup>1</sup> Photorefractive phenomenon have been studied for almost thirty years since their discovery in ferroelectric single crystals ( $\text{LiNbO}_3$ ) in 1966.<sup>2</sup> Since then, research on photorefractive effects has focused exclusively on inorganic materials, such as ferroelectric crystals ( $\text{LiNbO}_3$ ,  $\text{LiTaO}_3$ ,  $\text{BaTiO}_3$ ), semiconductors ( $\text{GaAs}$ ,  $\text{InP}$ ,  $\text{CdF}_2$ ) and sillenites ( $\text{Bi}_{12}\text{SiO}_{20}$ ).<sup>1-2</sup> Recently, organic single crystal and photorefractive polymers have emerged as new kinds of optical materials.<sup>3,4</sup> It is expected that PR polymers will possess unique properties supplemental to their inorganic counterparts: properties such as ease of preparation for large area samples, a low dielectric constant, high optical performance, and low cost.<sup>5</sup>

In the past several years, two approaches have been developed to prepare or synthesize photorefractive polymeric materials, namely, the composite material approach and the fully functionalized polymer approach.<sup>5-22</sup> Composite materials are composed of polymer hosts (electro-optic polymers, photoconductive polymers or inert polymers) doped with different functional molecules necessary for the photorefractive effect. Fully functionalized polymers are single-chain polymers which contain all of the functionality necessary for the photorefractive effect. Both approaches have enjoyed success in identifying photorefractive polymers. The materials performances have been greatly enhanced; for example, a diffraction efficiency of nearly 85% and an optical net gain of  $200\text{ cm}^{-1}$  was observed in a composite material. Prototype devices based on these materials were also attempted.<sup>24</sup>

Composite systems exhibit a major advantage. They make it easier to prepare different materials and to survey different compositions quickly. However, composite systems also exhibit several serious problems: such as intrinsic instability due to phase separation and low glass transition temperature. Although fully functionalized polymer systems exhibit several disadvantages, such as time-consuming chemical synthesis and difficulty in rational design, these polymers offer advantages that the composite materials do not possess, such as long term stability of the photorefractive effect and minimized phase separation. Therefore both approaches are necessary for the development of photorefractive polymers. However, judging from the development history of second order nonlinear optical (NLO) polymers, the functionalized polymer approach will be the preferred one.

Our research project sponsored by the Air Force Office of Scientific Research (Grant Number: F49620-93-1-0195) has been mainly involved in synthesizing fully functionalized PR polymers. Three polymer systems have been developed; functionalized polyurethanes, functionalized conjugated polymers and polyimides containing porphyrin and NLO chromophore units. The progresses in rational design, synthesis and characterization of fully functionalized photorefractive polymers is described in this final report.

## ***Part I: Photorefractive Polymers:***

### **Functionalized Polyurethanes.**

***Design and syntheses:*** Our initial idea to synthesize fully functionalized photorefractive polymers was simple: attaching four different species onto the polymer backbone. The design principle was based on the general view that in a photorefractive material, four functional species exist simultaneously: a photocharge generator, charge transporter, charge trapping centers and second order nonlinear optical moiety. In the first such polymer, we intentionally did not incorporate the charge trapping center. Trapping centers naturally exist in the polymer sample due to defects and conformational disorders.

Thus, only the NLO chromophore, the charge generator and the transporting compound were covalently linked to the polyurethane backbone. There are numerous compounds which can be chosen to play these three roles. When selecting different species, an important consideration is the absorption windows of different species. We chose the charge generator absorbing at long wavelengths (above 500 nm) so that a continuous diode laser could be used to excite the species. However, we chose a charge transporting compound and a NLO chromophore that absorb at short wavelengths. The purpose of this design was to avoid the excitation of the other species when the charge generator was excited, so that the physical properties of the charge transporter and NLO chromophore would not change. Figure 2 shows the monomer structures and their absorption maximum wavelengths.

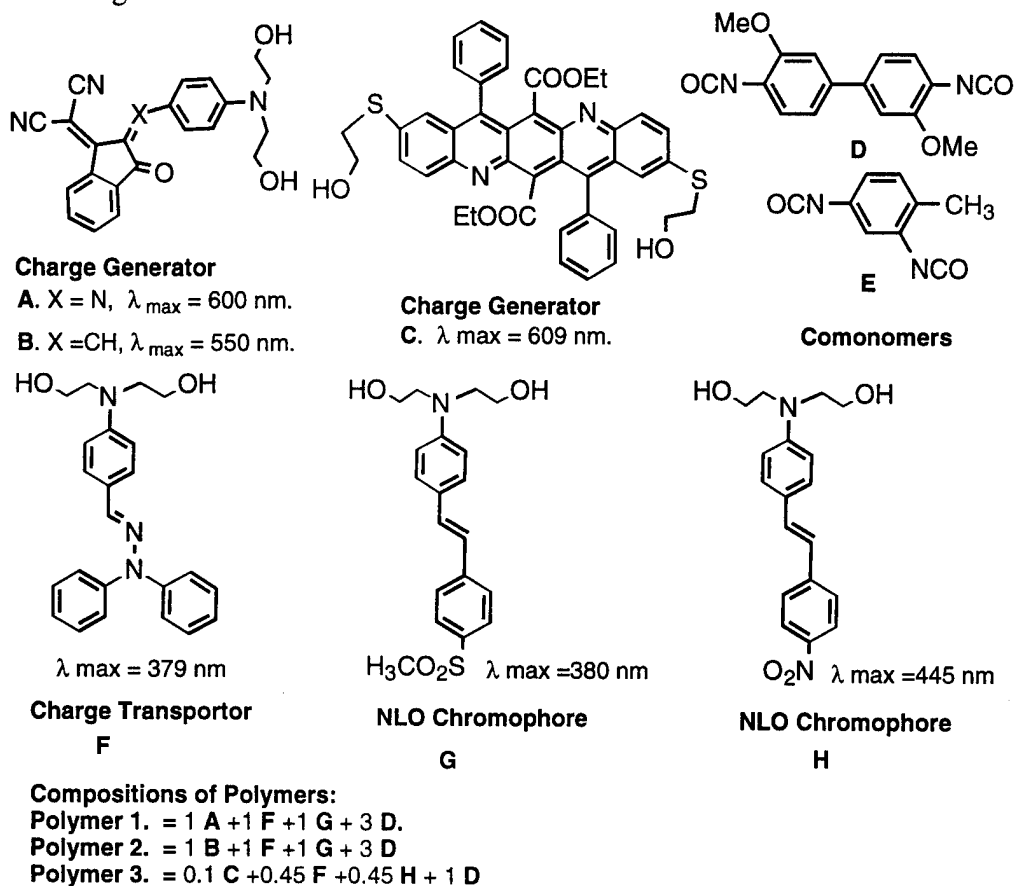


Figure 2. Structures and Absorption wavelengths of monomers and the compositions of polymers 1-3



The synthesis of the polyurethanes was straightforward and the structures of the resulting polymers were fully characterized (see Figure 2 for polymers' compositions). After polymerization, the maximum absorption wavelength of the charge generators did not change significantly, which indicated that no charge transfer complexes were formed between the charge generator and the various other species. The absorptions of the NLO chromophore and the transporting compound were similar to those of the corresponding monomers.

**Photoconductive studies:** In order to manifest the photorefractive effect, a polymer must possess two necessary properties: photoconductivity and electro-optical activity. Photoconductivity is required to achieve charge separation and the electro-optic response is needed to modify the index of refraction of the materials. All of the polymers 1-3 were found to be photoconductive. A maximum photocurrent of 1.5  $\mu\text{A}$  was observed for polymers 1 and 2 with an applied electric field of 1000 kV/cm and a laser intensity of 400 mW/cm<sup>2</sup> (at 632 nm). A photoconductivity of  $1.3 \times 10^{-13} \Omega^{-1} \text{cm}^{-1}$  for polymer 3 was obtained under a field strength of 290 kV/cm and a laser intensity of 270 mW/cm<sup>2</sup> (at 690 nm), corresponding to a quantum efficiency of the charge generation, ca.  $4.3 \times 10^{-7}$ . Just like other photoconductive polymers, the photocurrents of these polymers were both field and intensity dependent: as the field increased, the photoconductivity increased. A linear relationship between the photocurrent and the incident laser intensity was found, indicating that bimolecular recombination of the charge carrier was absent in this polymer system.

**Electro-optic effect:** The pristine polymer thin film has a random dipole orientation and exhibits no electro-optic response. However, if the dipoles of the NLO chromophores are aligned under an external electric field, the materials become asymmetric and thus electro-optically active. The most frequently used method is the corona discharging to electrically pole the polymer film when it is heated near the glass transition temperature. After that, the electro-optic effect in the polymer can be studied using a

continuous laser source. Electro-optic coefficients,  $r_{33}$ , of 12.2 and 13.0 pm/v were detected for polymers 1 and 2, respectively, at 632 nm. The linear E-O coefficient  $r_{33}$  of polymer 3 was determined to be 4.0 pm/V (thickness: 0.8  $\mu\text{m}$ ) at 690 nm. One of the advantages of these polymers is that their E-O coefficients are quite stable due to hydrogen bonding. For example, a  $r_{33}$  value of 11.6 pm/V was detected three months after poling for polymer 1.

**Two beam coupling experiments:** Possessing two necessary properties does not ensure the materials to be photorefractive. In order to confirm the photorefractive effect, a distinctive experiment, two-beam coupling, should be performed. As shown in Figure 1, when two coherent laser beams intersect upon the photorefractive polymers, an index grating can be generated, which can diffract these two beams into each other, leading to an asymmetric energy exchange characterized by the beam coupling coefficient,  $\Gamma$ .<sup>1</sup> By monitoring this optical energy exchange, one can deduce the optical gain coefficient from the equation<sup>1</sup>

$$\Gamma = \frac{1}{L} \ln \left( \frac{1+a}{1-\beta a} \right), \quad (1)$$

where  $a = \Delta I_s(L)/I_s(L)$ ,  $\Delta I_s(L)$  is the intensity change of the signal beam,  $I_s(L)$  is the total signal beam intensity emerging from the sample,  $L$  is the path length of the writing beam, and  $\beta = I_s(0)/I_p(0)$ , is the ratio of the incident beams intensity.

Two beam coupling experiments are performed in a setup shown in Figure 3 where the polymer film is tilted by an angle of  $\phi$  in order to have a nonzero effective E-O coefficient value,  $r_{\text{eff}}$ . For example, polymer 3 was studied by using a diode laser (690 nm, s polarized) as the light source with the sample tilted at 30°. The effect of the asymmetric optical energy exchange between the two beams is clearly demonstrated, (see the inset of Figure 4). When the two writing beams, beam S (signal beam) and beam P (pump beam), were overlapped in the sample, beam S (curve b) lost optical energy and beam P (curve c) gained optical energy. After the sample was rotated 180° around the rotation axis in the sample plate, the phenomena became reversed; beam S (curve d) gained

optical energy and beam P (curve e) lost energy. Unpoled samples showed no such phenomena. This experimental result indicates that this polymer was indeed photorefractive.

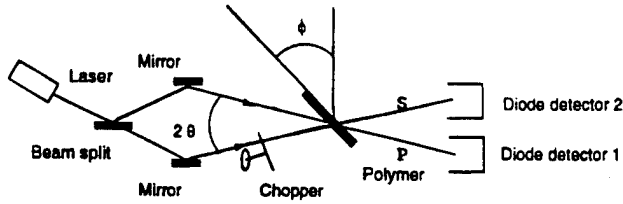


**Figure 3.** Experimental setup for two-beam coupling, where S and P are signal and pump beams.

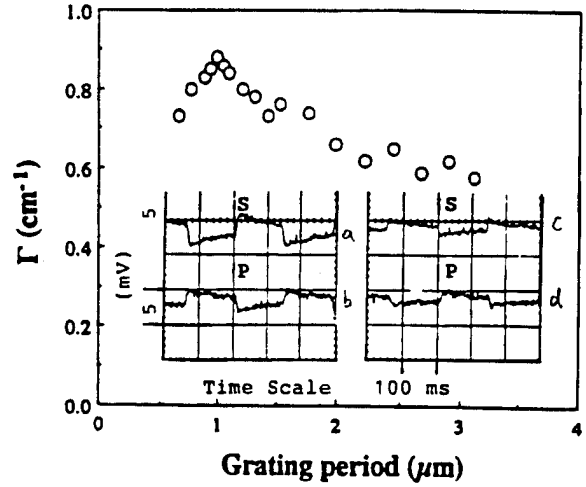


**Figure 4.** Optical gain coefficient,  $\Gamma$ , as a function of the grating period for polymer 3. The inset depicts the asymmetric energy exchange signals.

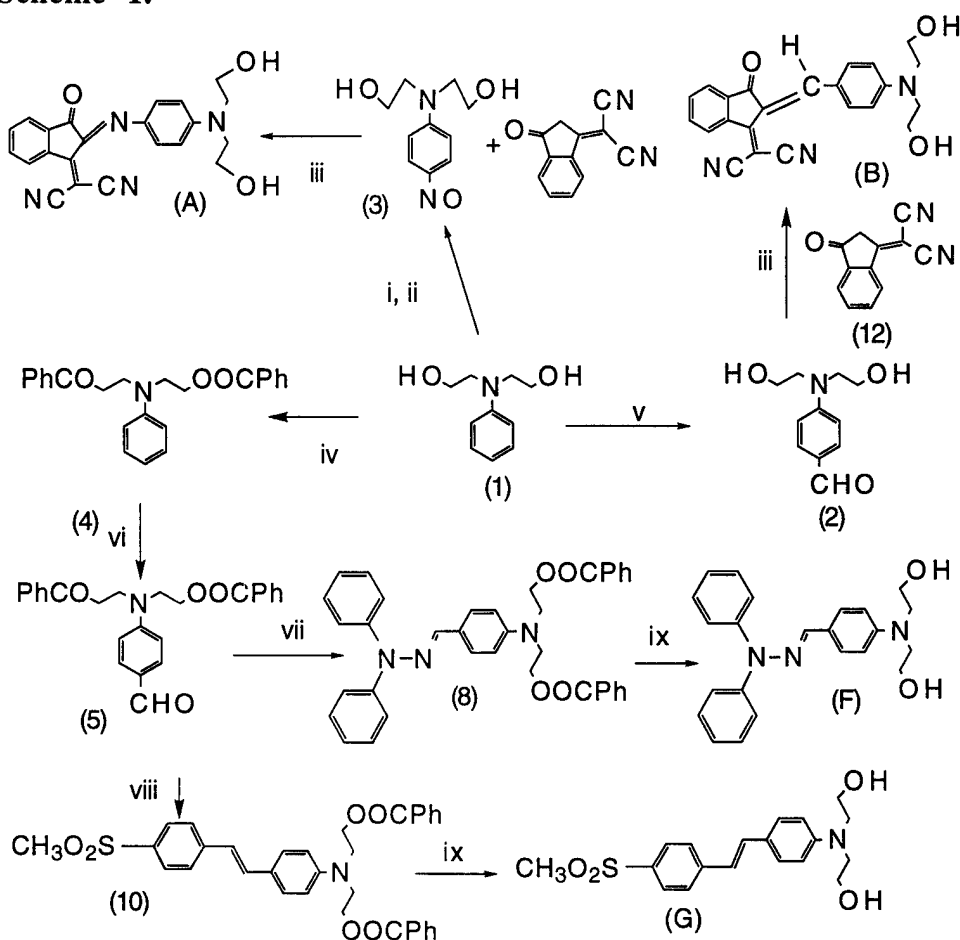
The optical gain results were measured as a function of the grating period ( $\Lambda = (\lambda/2\sin\theta)$ , Fig. 4). Two parameters characterizing the PR polymer, the effective density of the empty trap centers ( $N_e$ ) and the maximum refractive index change ( $\Delta n$ ), can be extracted. According to the band transport theory, the value of the grating spacing corresponding to the maximum optical gain is equal to the Debye screening length  $L_t = (4\pi^2\epsilon_0\epsilon k_B T/e^2 N_e)^{1/2}$ , where  $k_B$  is Boltzmann's constant. Thus, from the results of Fig. 4, an  $N_e$  value of ca  $2.3 \times 10^{14} \text{ cm}^{-3}$  was obtained. It is known that the maximum optical gain is related to  $\Delta n$  by  $\Gamma_{\max} = 4\pi\Delta n/\lambda\cos\theta$ , where  $\theta$  is the half interaction angle between the two writing beams. The value of  $\Gamma_{\max}$ ,  $0.88 \text{ cm}^{-1}$ , from Fig. 4, leads to a  $\Delta n$  of  $1 \times 10^{-5}$ .

For polymers 1 and 2, the two beam coupling experiments were carried out in a waveguide structure using a HeNe laser. In this experiment, the E-O coefficient tensor component,  $r_{51}$ , was utilized. The largest optical gain coefficient under a zero external field is  $2.3 \text{ cm}^{-1}$  at a grating wavenumber of  $0.6 \times 10^5 \text{ cm}^{-1}$ .

It is worth mentioning that although these polymers are indeed photorefractive, the observed optical gain under zero field conditions is not a net gain because of the strong absorption. There are also several common features in those functionalized polyurethanes. First, a comonomer (diisocyanate in this case) was used to link the different species; therefore, the density of the different species is limited to a low level. To optimize the PR effect, the densities of the charge transporter and the NLO chromophore should be optimized. In the above polymer systems, this could not be done simultaneously. Second, the polymer backbones were polyurethanes which cannot effectively transport the photocharge carriers. Third, since it is a copolymer with three functional species, their molecular weight is very difficult to optimize. Any impurities or weighing errors in monomers can lead to the miss-match of the monomers' stoichiometry which will lower the molecular weight. These are the reasons that the second type of PR polymers were designed, which contain a conjugated backbone and a second order NLO chromophore.

**Synthesis of Monomers:** N,N-benzocarboxyethyl aniline (**Compound 4**). Benzyl chloride (38.4 ml, 0.34 mol) was added dropwise to a solution of N,N-ethanol aniline (30 g, 0.17 mole) and triethylamine (60 ml) in THF (150 ml). The resulting mixture was stirred at room temperature for two hours and then poured into water (500 ml). A yellow oily liquid precipitated and solidified on standing. The solid was filtered off and recrystallized from methanol to yield white crystals (58.6 g, 91%, m.p.72.0-73.5°C ).  $^1\text{H}$  NMR ( $\text{CDCl}_3$ ),  $\delta$  (ppm), 3.82, (t,  $J = 6.6$  Hz, 4 H,  $-\text{NCH}_2-$ ), 4.52, (t,  $J = 6.6$  Hz, 4 H,  $-\text{CH}_2\text{O}-$ ), 6.71-7.97 (m, 15 H, aromatic protons).

**Scheme 1.**



**Reaction Conditions**

- i. NaNO<sub>2</sub>, HCl ii. Na<sub>2</sub>CO<sub>3</sub> iii. EtOH/CH<sub>2</sub>Cl<sub>2</sub> iv. PhCOCl, NEt<sub>3</sub>  
 v. (CH<sub>2</sub>NH)<sub>6</sub>, HCOOH, EtOH vi. DMF, POCl<sub>3</sub> vii. Ph<sub>2</sub>NNH<sub>2</sub>, NaOAc  
 viii. (CH<sub>3</sub>O<sub>2</sub>S)-Ph-CH<sub>2</sub>P(O)(OEt)<sub>2</sub>, NaH, glyme; ix. NaOH/H<sub>2</sub>O/EtOH

*N,N*-bezocarboxyethyl aminobenzaldehyde (**Compound 5**). Phosphorus oxychloride (4.79 ml, 51.4 mmol) was added dropwise to DMF (10 ml) at 0 °C and the resultant solution was stirred for 1 hr at 0 °C and for another 1 hr at 25 °C. Compound 4 (20 g, 51.4 mmol) in DMF (10 ml) was then added slowly to the solution and the mixture was further heated at 90 °C for 6 hr. After the completion of the reaction, the mixture was poured into crushed ice (50 g) and extracted with methylene chloride three times (a portion of 50 ml). The organic layer was washed with a saturated sodium bicarbonate solution,

water (twice), and dried over magnesium sulfate. The solvent was removed under reduced pressure. The crude product was recrystallized from methanol, obtaining a white solid, (16.7 g, 78%, m.p. 78.0-79.5°C ). <sup>1</sup>H NMR, (CDCl<sub>3</sub>), δ, (ppm), 3.93, (t, J = 5.9, 4 H, -NCH<sub>2</sub>-), 4.56, (t, J = 5.9, 4 H, -CH<sub>2</sub>O-), 6.94-7.99, (m, 14 H, aromatic protons), 9.76, (s, 1 H, -CHO).

**Monomer A.** A mixture of 4-nitroso-NN'diethanolaniline (3.500g, 16.67mmol) and 3-dicyanovinylindan-1-one (compound 12, 3.000g, 15.96 mmol) in ethanol /methylene chloride (20 ml/10 ml) was stirred at room temperature for 5 hr. The suspension was filtered and the solid was washed with ethanol until the filtrate turned blue. The product was recrystallized from ethanol (4.78g, 84% based on compound 12, m.p. 216-218°C). <sup>1</sup>H NMR (DMSO-d<sub>6</sub>), δ, (ppm), 3.6-3.7, (m, 8 H, -CH<sub>2</sub>CH<sub>2</sub>-), 4.8 (t, J= 4 Hz, 2 H, OH), 6.95-8.5, (m, 8 H, aromatic protons). Mass spectrum: M<sup>+</sup>/Z, 386, 368, 355, 296. Anal. Calcd. for (C<sub>22</sub>H<sub>18</sub>N<sub>4</sub>O<sub>3</sub>): C, 68.39, H, 4.66, N, 14.51% Found, C, 68.57, H, 5.01, N, 14.43%.

**Monomer B.** This compound was synthesized from N,N'diethanolaminobenzaldehyde and 3-dicyanovinylindan-1-one in a procedure similarly used for Monomer A. <sup>1</sup>H NMR, (DMSO-d<sub>6</sub>), δ, (ppm), 3.6-3.8, (m, 8 H, -CH<sub>2</sub>CH<sub>2</sub>-), 6.95-8.5, (m, 9 H, aromatic and vinyl protons). Anal. Calcd. for (C<sub>23</sub>H<sub>19</sub>N<sub>3</sub>O<sub>3</sub>): C, 71.69, H, 4.94, N, 14.61; Found, C, 71.54, H, 4.87, N, 14.72%.

**Monomer F.** A mixture of compound 5 (6.00g, 20 mmol), 1,1-diphenylhydrazine hydrochloride (0.44g, 20 mmol), sodium acetate (1.8g, 22 mmol) and ethanol (50 ml) was stirred at room temperature for 2 hr. A sodium hydroxide solution (20%, 20 ml) was added and the reaction mixture was further stirred at room temperature overnight. The product crystallized out during stirring and was filtered off. After washing it with water three times, the solid was recrystallized from methanol, (6.5 g, 72%, m.p., 124.5-125.5 °C). <sup>1</sup>H NMR spectrum (DMSO-d<sub>6</sub>) δ (ppm), 3.4, (t, J = 6 Hz, 4 H, -NCH<sub>2</sub>-), 3.6, (t, J = 6 Hz, 4 H, OCH<sub>2</sub>-), 4.75 (t, J = 4 Hz, 2 H, OH), 6.6-7.4 (m, 15 H,

Aromatic proton and  $-\text{CH}=\text{N}-$ ). Mass spectrum,  $M^+/Z = 375, 357, 344, 169$ . Anal. Calcd. for  $(\text{C}_{23}\text{H}_{25}\text{N}_3\text{O}_2)$ : C, 73.60, H, 6.67, N, 11.20%; Found, C, 73.35, H, 6.76, N, 11.06%.

**Monomer G.** This compound was prepared according to the literature procedure with some modifications.<sup>10</sup> In a 250 ml round flask flushed with nitrogen, the mixture of compound 5 (14.53 g, 34.8 mmol), sodium hydride (2.50 g, 104.0 mmol) and 1,2-dimethoxyethane (glyme, 80 ml) was stirred for 5 min. To this solution was added diethyl-4-(methylsulfonyl)benzylphosphonate (10.65 g, 34.8 mmol) in glyme (40 ml). The resultant mixture was heated under reflux for 2 hr and then poured over crushed ice (200g) under nitrogen. The viscous material was isolated and dissolved in ethanol (60 ml). To this solution was added a sodium hydroxide solution (4 g in 15 ml of water) and the mixture was heated to reflux overnight. After cooling, the yellow solid was filtered off and washed with water three times. The crude product was further recrystallized from methanol, (3.49, 28%, m.p.278-280°C).  $^1\text{H}$  NMR ( $\text{DMSO}-d_6$ ),  $\delta$  (ppm), 3.1, (s, 3 H,  $-\text{SO}_2\text{CH}_3$ ), 3.4, (t,  $J = 6$  Hz, 4 H,  $-\text{NCH}_2-$ ), 3.6, (t,  $J = 6$  Hz, 4 H,  $\text{OCH}_2-$ ), 4.75 (t,  $J = 4$  Hz, 2 H, OH), 6.7, 7.4, 7.7, 7.8, (m, 8 H, aromatic Proton), 7.0 and 7.3, (d, 10 Hz, 2 H, Vinyl proton). Mass spectrum:  $M^+/Z = 361, 343, 330, 300, 286, 207, 178$ . Anal. Calcd. for  $(\text{C}_{19}\text{H}_{23}\text{NO}_4\text{S})$ , C, 63.16, H, 6.37, N, 3.88%. Found: C, 62.96, H, 6.71, N, 3.59%.

**Polymerization:** In a typical polymerization, a mixture of monomers A (0.3208 g, 0.831 mmol), F (0.3116 g, 0.831 mmol), G (0.3000g, 0.831 mmol) and 3,3'-dimethoxy,4,4'-diisocyanate-bisphenyl (monomer D, 0.7380 g, 2.493 mmol, as comonomer) was dissolved in DMF (20 ml) and two drops of triethylamine was added to facilitate the polymerization. The resultant mixture was heated to 90°C for 2 hr. and was then poured into methanol. The polymer was filtered off and washed with methanol until colorless. It was further purified by extraction in a soxhlet extractor with methanol under the wrap of aluminum foils. Then it was dried under a vacuum at 50°C for two days.

**Physical measurements:** After spin coating the polymer onto an indium-tin-oxide (ITO) glass slide, gold electrodes were deposited on the polymer surface. Photoconductivity measurements were performed by monitoring the photocurrent response of the polymer sample (90  $\mu\text{m}$ ) to a laser beam at 632 nm with an intensity of 0.4 W/cm<sup>2</sup>. The electro-optic effect in the polymer was studied by using an interferometry method at 632 nm.<sup>11</sup> The dielectric constant was determined by measuring the capacitance of the ITO-Polymer-Gold structure as described in the literature.<sup>12</sup>

In order to characterize the mechanism of the photoinduced grating in the polymers, two beam coupling experiments were performed. Due to the difficulties of fabricating a polymer film of uniform thickness, a planar waveguide geometry was chosen to increase the grating interaction length. The experimental setup is shown in Figure 1 where a HeNe laser is used as the light source. The output of the HeNe laser was split into two beams of equal intensity. These two parallel collimated beams were simultaneously coupled into the polymer planar waveguide by a prism and intersected with each other with an angle of  $2\theta$  inside the waveguide. Finally, the two separated beams were coupled out of the polymer waveguide by another prism and sent into two calibrated photodiodes. The combined prisms and waveguide coupling apparatus was mounted on a piezo electrically driven translation stage and a step motor driven rotation stage. The polymer waveguides consisted of a 0.8  $\mu\text{m}$  thick spin-coated polymer film on an ITO glass substrate with a 100 nm thick SiO<sub>2</sub> buffer layer. The experiments were performed on both poled and unpoled samples.

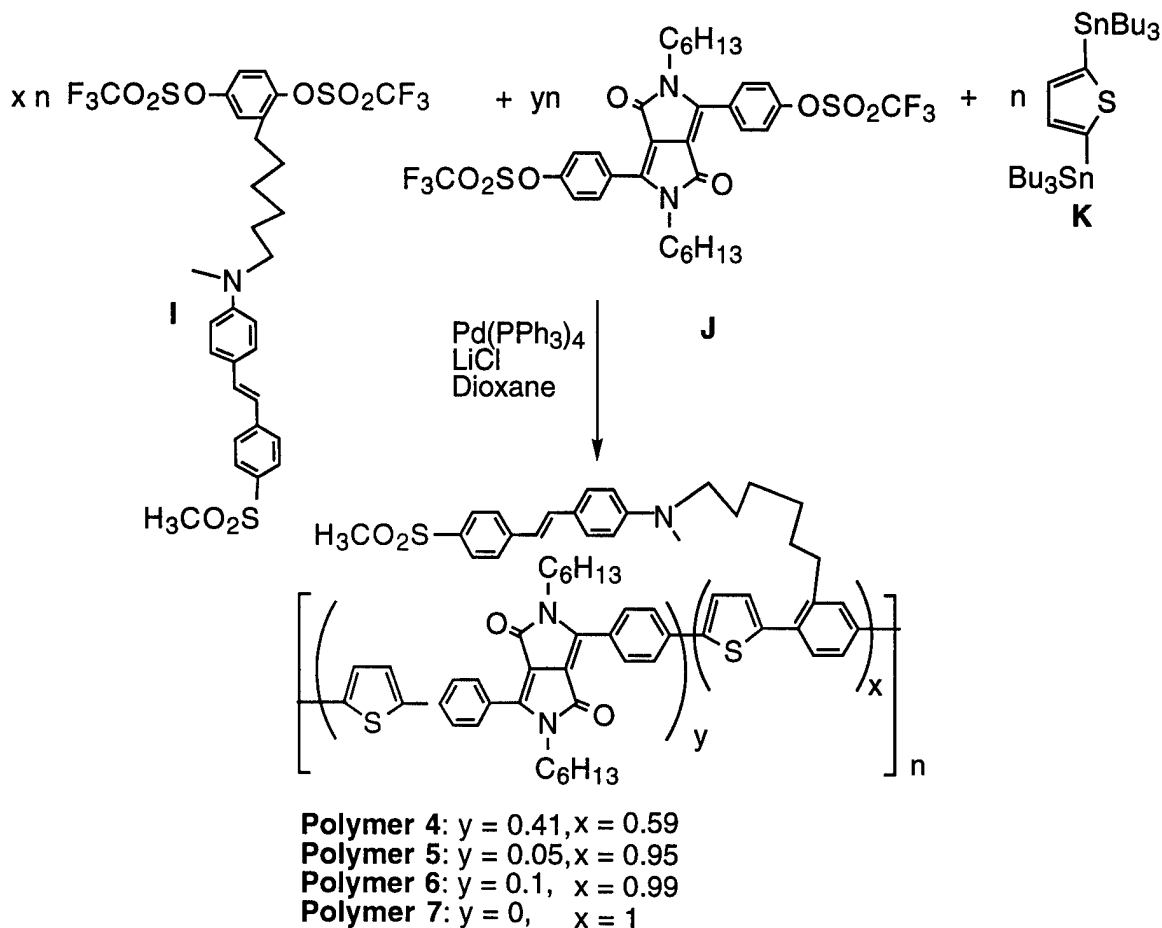
### **Functionalized Conjugated Polymers**

**Design ideas and syntheses:** The rationale for designing these new materials was that the conjugated backbone absorbs photons in the visible region and plays the triple role of charge generator, charge transporter and backbone. It is known that conjugated polymers have relatively high photo-generated carrier mobilities ( $10^{-3}$ - $10^{-5}$  cm<sup>2</sup>/Vs).<sup>30</sup>



Thus, the four functions necessary to manifest the PR effect exist simultaneously in a single polymer. Furthermore, the use of conjugated backbones enhances the density of the NLO chromophores.

**Scheme 2.**



However, in order to synthesize these polymers, a new polymerization approach needs to be developed because these polymers contain many functional groups which may not be tolerated in many polymerization processes, such as Zigler-Natta polymerization,<sup>31</sup> electrochemical polymerization and the oxidative coupling reaction.<sup>32</sup> Fortunately, we have found that the Stille coupling reaction, a palladium-catalyzed reaction between organic halides (or triflate) and organotin compounds, offers the solution to this problem.<sup>33-35</sup> The reaction requires very mild conditions and can tolerate different substituents of monomers, such as amines, esters, ethers, etc., allowing us to introduce different functionality into the polymer backbone. The structure of the synthesized conjugated

photorefractive polymers is shown in Scheme 2 (polymers **4** to **7**). We introduced the dihydropyrrolopyrroldione (DPPD) compound as the photosensitizer to extend the photosensitive region into a longer wavelength. These types of compounds have strong absorptions in the visible region.

The polymerization went smoothly while a typical Stille catalyst system was used. Either  $\text{Pd}(\text{PPh}_3)_4$  with  $\text{LiCl}$  or  $\text{Pd}(\text{PPh}_3)_2\text{Cl}_2$  alone can be used as the catalyst. Four polymers were synthesized with various compositions. These polymers were fully characterized by various spectroscopic and other techniques. The results were all consistent with the proposed polymer structures.

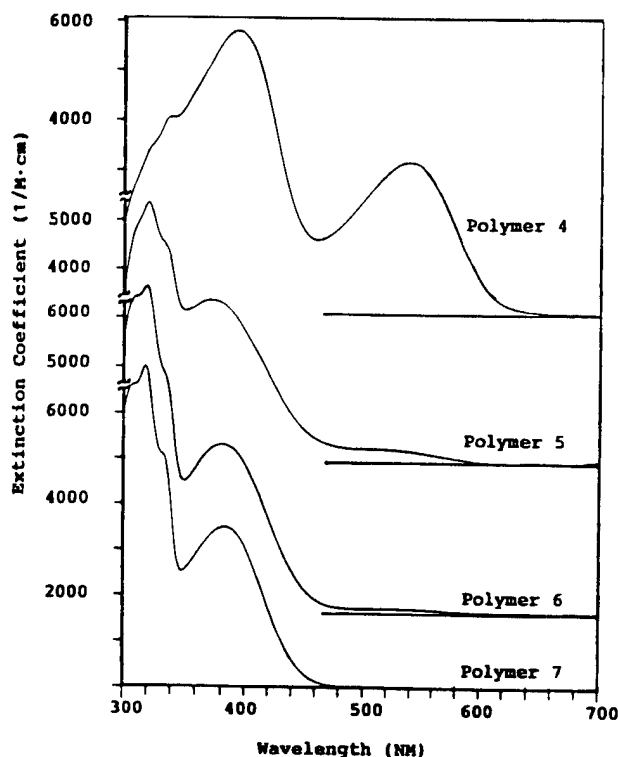


Figure 5. UV/vis spectra of polymers 4–7 in THF.

As the composition changed, the UV/vis spectral features of the polymers also changed. It can be noted that polymer **7** has an absorption at ca 390 nm, mainly due to the absorption of the NLO chromophore. Polymers **4** and **6**, however, show absorptions at

573 nm, which is dramatically shifted from the absorption of monomer **J** (483 nm). This illustrates clear evidence for the incorporation of the DPPD unit into the polymers. The absorption strength correlates well with the concentration of the DPPD units (Figure 5). These results indicate that we can control the absorption strength of the polymers at specific regions. This is very important for the design of photorefractive polymers. In order to demonstrate the photorefractive effect, the materials must have certain but small absorptions at the wavelength of a working laser, otherwise, either charge carrier can not be generated or the materials are too absorbing. For this reason, polymer **5** has been studied in detail.

As we pointed out at the beginning, there are four processes involved in the photorefractive effect, namely, charge generation, charge transporting, charge trapping and grating formation. In the present polymer system, the role of charge trapping is played by the defects existing in the polymer. Detailed studies regarding the trapping process were difficult before the exact nature of the trapping centers was known.

**Charge generation:** Photoconductivity studies of these polymers showed a strong dependence on the external field strength. As the electrical field was increased, the photocurrent initially increased linearly (Ohmic behavior) and then almost quadratically. A typical photocurrent response time of ca. 100 ms was estimated. A photoconductivity of  $1.8 \times 10^{-11} \Omega^{-1} \text{cm}^{-1}$  was obtained for polymer **5** under a field strength of 1500 kV/cm and a laser intensity of 311 mW/cm<sup>2</sup>. The photoconductivities for polymers **4** and **6** were found to be ca.  $8 \times 10^{-11}$  and  $4 \times 10^{-11} \Omega^{-1} \text{cm}^{-1}$ , respectively. These values are comparable to those of well known conjugated polymers, such as poly(phenylene-vinylene).<sup>37,38</sup> The photocurrent of polymer **5** was also measured as a function of several wavelengths of excitation at the same laser intensity (48 mW/cm<sup>2</sup>) and electric field (400 kV/cm). It was found that the spectral dependence of the photocurrent had a similar shape to the absorption spectrum of the conjugated PR polymer. This seemed to indicate that the optical excitation of the conjugated backbone was the origin of the photocharge generation.

The quantum yields of the photogeneration of charge carriers evaluated from the photocurrent results are listed in Table I, which is much larger than the polyurethane system. They showed the electric field dependence which can be theoretically simulated by Onsager's model of the geminate-pair dissociation.<sup>39</sup> The simulation results generated the two parameters from the best fitting,  $\eta_0$  (the yield of the thermalized bound pairs, independent of field), and  $r_0$  ( $= e^2/4\pi\epsilon_0\epsilon kT$ , the Onsager distance), which were 0.02 and 15 Å, comparable to the known conjugated polymers and the photoconductive polymers.<sup>27,37</sup> The  $r_0$  was also known to relate to the activation energy  $E_A$  at low field conditions<sup>38</sup>

$$r_0 = e^2/4\pi\epsilon_0\epsilon E_A. \quad (2)$$

Temperature dependent measurements of the carrier mobility indicated an activation energy of 0.16 eV for this polymer. The  $r_0$  was then calculated to be 18 Å, in agreement with experimental fitting results.

**Table 1.** Summary of the Physical Properties of Polymers 4 to 6.

Polymers	$\alpha$ (cm <sup>-1</sup> )	$d_{33}$ (pm/V)	$r_{33}$ (pm/V)	$\Phi$ (at 400 kV/cm)
<b>4</b>	242	54	4	$7 \times 10^{-4}$
<b>5</b>	201	89	10	$3 \times 10^{-4}$
<b>6</b>	137	90	10	$1.5 \times 10^{-4}$

**Charge transporting:** The charge carrier mobility ( $\mu$ ) is an important parameter for characterizing the charge transporting process. We used the time-of-flight (TOF) technique to determine the charge carrier mobility. The results showed a dispersive charge transport as indicated by the initial decay and the tail of the transient signals. The temperature-dependent measurements of the charge carrier's mobility indicate that the charge transporting process is thermally activated with an Arrhenius activation energy of 0.16 eV and 0.23 eV for polymers **5** and **4**, respectively. The field dependence of the carrier mobility was anomalous; as the field was increased, the mobility decreased. Similar

phenomena were observed in the poly(2-phenyl-1,4-phenylene-vinylene) systems,<sup>38</sup> and in a few composite photoconductive systems.<sup>40</sup> It was attributed to the random walk of the charge carrier within a random potential field.<sup>38</sup> The randomness of the potential field in this polymer was manifested by the broadened absorption spectrum (Figure 5).

**Electro-optic Effect:** The E-O coefficients were measured according to the method described in reference.<sup>28</sup> The results are shown in Table I. Compared to the polyurethane systems, these polymers are less stable in E-O response; a gradual decay (to 80% of initial value after 100 hours) was observed for all of these polymers.

**Optical gain and photorefractive grating:** Two beam coupling experiments were performed to characterize the photorefractivity of the polymers. The asymmetric optical energy exchange is shown in the inset of Figure 6. The resulting  $\Gamma$  values for polymer 5 are plotted as a function of the grating wavenumber ( $K = 4\pi \sin\theta/\lambda$ ) in Fig. 6. Similar results were obtained for polymers 4 and 6. Two parameters characterizing PR polymer 5, the effective density of the empty trap centers ( $N_e$ ) and the maximum refractive index change ( $\Delta n$ ), extracted from Figure 6, are ca.  $2 \times 10^{14} \text{ cm}^{-3}$  and  $4 \times 10^{-5}$ , respectively. For polymer 4, an  $N_e$  of ca.  $1.9 \times 10^{15} \text{ cm}^{-3}$  and a  $\Delta n$  of  $3 \times 10^{-5}$  were deduced.

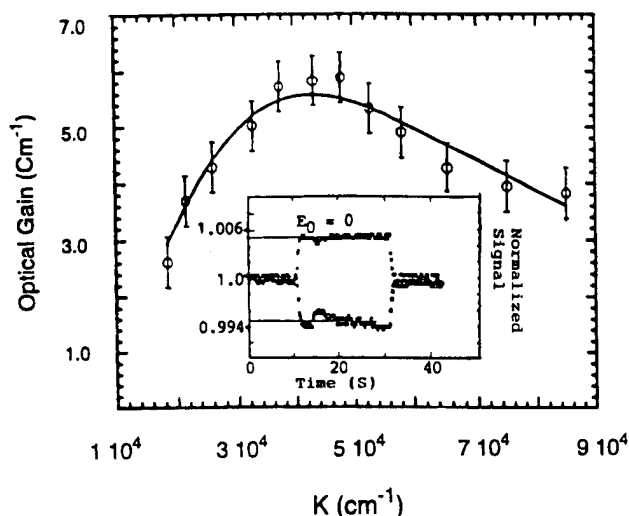


**Figure 6.** Optical gain coefficient,  $\Gamma$ , as a function of the grating wavenumber for polymer 5. The inset depicts the asymmetric energy exchange signals under a zero field.

The refractive index change is related to the space-charge field by  $\Delta n = n^3 r_{\text{eff}} E / 2$ , where  $r_{\text{eff}}$  is the effective electro-optic coefficient. The large index change ( $\Delta n \sim 7.1 \times 10^{-5}$ ) under zero field conditions implied either a large space charge field ( $\sim 100$  kV/cm) or a large electro-optical coefficient (200 pm/V). Both implications are in contrast to the theoretical expectations and with the results obtained by independent measurements. According to the photorefractive theory based on the band transport model, the largest space charge field which can be achieved under zero-field conditions is the thermal diffusion field  $E_d = k_B T K / e$  ( $\sim 1.37$  kV/cm).<sup>1</sup> The experimental value of the E-O coefficient for this polymer was about 2-4 pm/V (Electrode poling). These discrepancies implied that there are other factors responsible for such a large optical gain. A reasonable assumption is that an internal field existed which assisted the charge separation and enhanced the photorefractivity under a zero-field. This assumption has a solid base because of the orientation of the dipoles of the nonlinear optical chromophore after electric poling.

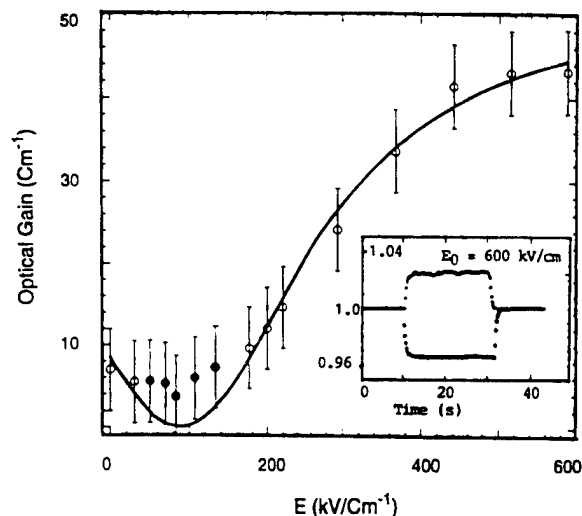


**Figure 7.** Optical gain coefficient,  $\Gamma$ , as a function of the external electric field for polymer 5. The inset depicts the asymmetric energy exchange signals under an electric field of 600 kV/cm.

Further evidence for the existence of the internal field was obtained from the field dependent studies of the optical gain. It was found that the optical gain decreased when increasing the field in the region of 0 - 100 kV/cm, and there existed a flat valley near the field of  $10^2$  kV/cm (Figure 7). The optical gain increased as the field further increased. The results indicated that the internal field was about  $10^2$  kV/cm opposite the direction to the poling field. Many further measurements gave results with more clear trends which are consistent with the suggested internal field.

Theoretical fitting was carried out based on the relationship between the optical gain and the space charge field ( $E_{sc}$ ):<sup>1</sup>

$$\Gamma = \frac{\pi n^3 \sin \phi \, r_{\text{eff}} E_{sc}}{\lambda \, m \cos \theta} = \frac{\pi n^3}{\lambda \cos \theta} \sin \phi \, r_{\text{eff}} E_q \sqrt{\frac{E_0^2 + E_d^2}{E_0^2 + (E_d + E_q)^2}}, \quad (3)$$

with

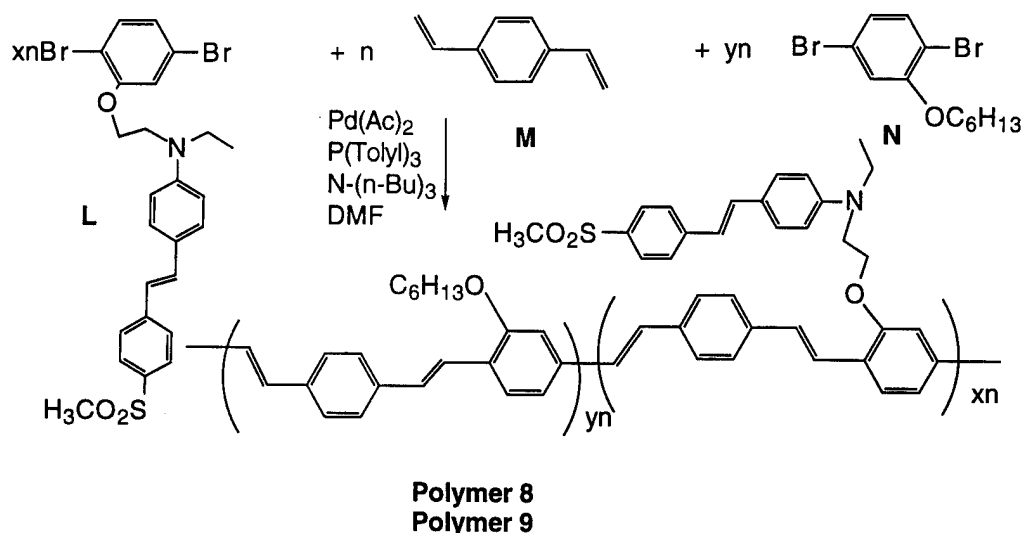
$$\phi = \tan^{-1} \left[ \frac{E_d}{E_0} \left( 1 + \frac{E_d}{E_q} + \frac{E_0^2}{E_d E_q} \right) \right], \quad (4)$$

where  $\phi$  is the phase shift between the interference pattern and the index grating,  $r_{\text{eff}}$  is the effective E-O coefficient,  $E_d = k_B T K / e$  is the diffusion field,  $E_q = e N_e / \epsilon_0 \epsilon K$  is the limiting space charge field,  $E_0$  is the external electric field,  $\epsilon$  is the dielectric constant (4.85), and  $N_e$  is the effective density of the empty trap centers. By incorporating the internal field term, the  $E_0$  term in the above equation becomes  $\sin \theta (E^* + E_i)$ , where  $\theta$  is the angle between the grating wave vector and the sample plane ( $30^\circ$ ),  $E^*$  is an applied field (0 - 588 kV/cm), and  $E_i$  is an internal field. The simulation of the field dependent data according to equations 11 and 12 yielded  $E_q = 1.0 \times 10^2$  kV/cm,  $E_i = 8.8 \times 10^2$  kV/cm and  $r_{\text{eff}} = 1.0$  pm/V. The extracted value of  $E_i$  from the fitting was very interesting and in reasonable agreement with the value evaluated theoretically in other polar polymer systems.<sup>41</sup>

It is known that there are many different types of conjugated polymers which can be explored through photorefractive studies. An obvious extension is to utilize other conjugated polymer backbones, such as poly(phenylenevinylene) (PPV) which exhibits high photoconductivity. Studies by us and other groups also indicate that PPV backbones

are easy to functionalize by utilizing the Heck coupling reaction.<sup>42</sup> Two dibromobenzene derivatives substituted with an NLO chromophore and an alkoxy group were used as monomers. These monomers were copolymerized with *p*-divinylbenzene to give the resulting copolymers (Scheme 3). However, detailed photorefractive studies revealed that although the copolymer possessed both photoconductivity and electro-optic response, the polymer systems exhibited no positive results for the photorefractive phenomenon. This is one example which shows the complication in designing PR polymers; the existence of two necessary physical properties in a single polymer does not sufficiently ensure that the polymer will be photorefractive. Similar phenomenon were observed in a composite PR material (Polyvinylcarbazole:2,4,7-trinitro-9-fluorenone:2-(4-nitrophenyl)-4,5-bis(4-methoxyphenyl)imidazole).

**Scheme 3:**

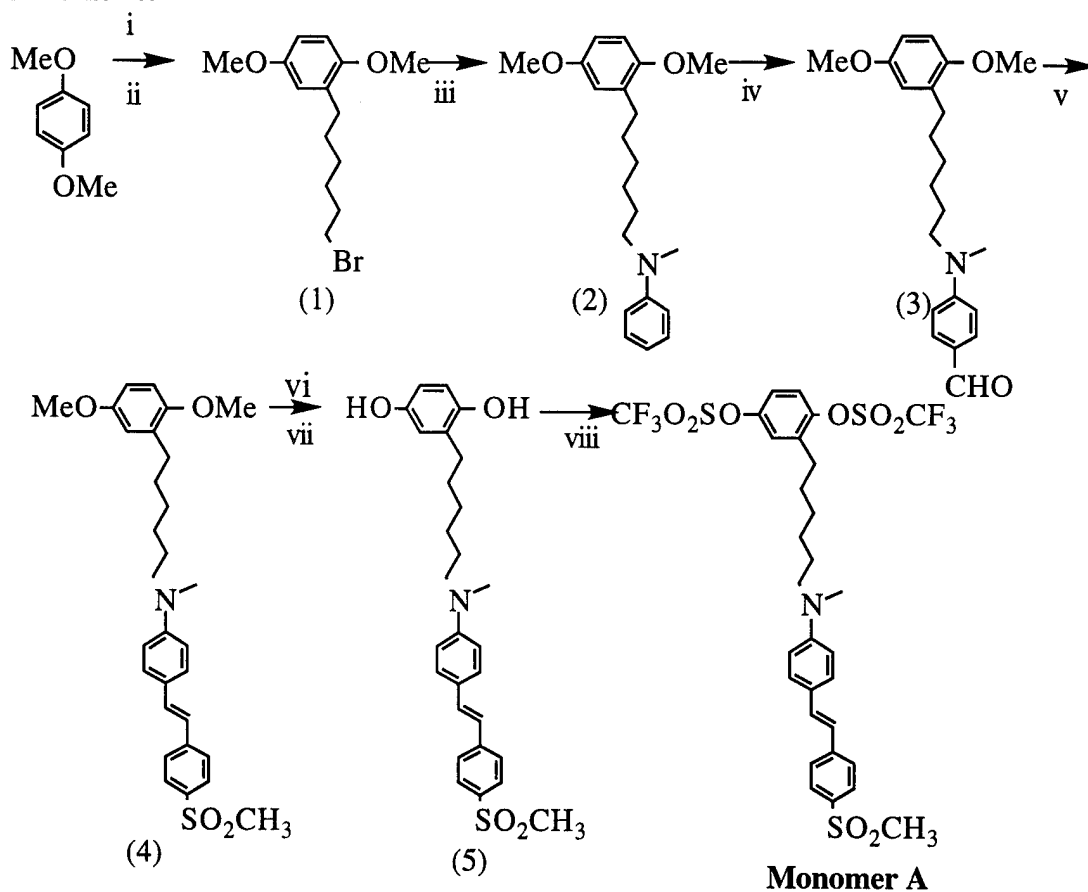


**Synthesis of Monomers:** **Compound 1.** n-Butyl lithium (2.5M, 68 ml, 171 mmol) was added to a solution of 1,4-dimethoxybenzene (23.6 g, 171 mmol) in THF (40 ml) in a 500 ml two necked round bottom flask at 0 °C. The solution was stirred for 1 hr and was then transferred dropwise into a solution of 1,6-dibromohexane (33.2 ml, 205 mmol) in THF(20 ml) in another round bottom flask. The resulting mixture was stirred at room temperature for 1 hr. and was then poured into water (100 ml). The mixture was



extracted with diethyl ether (3 x 30 ml); the organic layers were combined, washed with a saturated sodium chloride solution (30 ml) and dried over magnesium sulfate. After removal of the solvent, the crude product was vacuum distilled to yield a colorless liquid, compound 1 (28.5 g, 55%); b.p. 155-160°C (1 Torr).  $^1\text{H}$  NMR ( $\text{CDCl}_3$ , ppm):  $\delta$  1.34-1.86 (m,  $-\text{C}_4\text{H}_8-$ , 8 H), 2.56 (t,  $J = 7.6$  Hz,  $\text{Ar}-\text{CH}_2-$ , 2 H), 3.38 (t,  $J = 6.8$  Hz,  $\text{Br}-\text{CH}_2-$ , 2 H), 3.74 (s,  $\text{CH}_3\text{O}-$  3 H), 3.75 (s,  $\text{CH}_3\text{O}-$ , 3 H), 6.63-6.73 (m,  $\text{ArH}$ , 3 H).

**Scheme 4:**



**Reaction conditions:**

i.  $\text{LiBu}/\text{THF}$ , ii, 1,6-dibromohexane, iii,  $\text{N-methylaniline}/\text{NBu}_4\text{Br}/\text{Na}_2\text{CO}_3/\text{Toluene}$ , iv.  $\text{POCl}_3/\text{DMF}$ , v, diethyl 4-(methylsulfonyl)benzyl phosphate/ $\text{NaH}/\text{Glyme}$ , vi,  $\text{BBr}_3/\text{CH}_2\text{Cl}_2$ , vii,  $\text{H}_2\text{O}$ , viii, Pyridine/trifluoromethanesulfonic anhydride.

**Compound 2:** In a 100 ml round bottom flask, a solution of compound 1 (10.00 g, 33.2 mmol),  $\text{N-methylaniline}$  (5.40 ml, 49.8 mmol), potassium carbonate (9.20 g, 66.4 mmol), tetrabutylammonium bromide (0.54 g, 1.7 mmol) and sodium iodide (10 mg, 0.07

mmol) in toluene (10 ml) was stirred under reflux for 5 hr. Diethyl ether (25 ml) and water (25 ml) were added. The organic layer was separated and dried over magnesium sulfate. After removal of the solvent, the unreacted starting material was distilled out under a vacuum (50 °C, 1 torr); compound 2 was collected as a residue (10.00 g, 92%). <sup>1</sup>H NMR (CDCl<sub>3</sub>, ppm): δ 1.34-1.58 (m, -C<sub>4</sub>H<sub>8</sub>-, 8 H), 2.55 (t, J = 6.3 Hz, Ar-CH<sub>2</sub>-, 2 H), 2.87 (s, N-CH<sub>3</sub>, 3 H), 3.25 (t, J = 6.7 Hz, -NCH<sub>2</sub>-, 2 H), 3.71(s, CH<sub>3</sub>O-, 3 H), 3.72 (s, CH<sub>3</sub>O-, 3 H), 6.61-6.70 (m, ArH, 6 H), 7.14-7.17 (m, ArH, 2 H).

**Compound 3:** Phosphorus oxychloride (1.4 ml, 15.3 mmol) was added dropwise to DMF (4.7 ml, 61.2 mol) at 0°C. The solution was stirred at 0°C for 1 hr and then at 25°C for another 1 hr. Compound 2 (5.00 g, 15.3 mmol) was then added dropwise to the mixture. The resulting solution was stirred at 90°C for 4 hr. After being cooled down to room temperature, the solution was poured into an ice-water mixture. It was neutralized with a saturated sodium acetate solution. The mixture was extracted with dichloromethane (3 X 20 ml). The combined organic solution was washed with water (2 X 25 ml) and then with a saturated sodium chloride solution (25 ml). After removal of the solvent, the crude product was chromatographed using a silica gel column, using hexane/ethyl acetate (2:1) as the eluent, affording a pale yellow liquid compound 3 (2.40 g, 45%). <sup>1</sup>H NMR (CDCl<sub>3</sub>, ppm): δ 1.34-1.58 (m, -C<sub>4</sub>H<sub>8</sub>-, 8 H), 2.56 (t, J = 6.3 Hz, Ar-CH<sub>2</sub>-, 2 H), 3.01 (s, NCH<sub>3</sub>, 3 H), 3.37 (t, J = 7.5 Hz, NCH<sub>2</sub>-, 2 H), 3.73 (s, -OCH<sub>3</sub>, 3 H), 3.74 (s, -OCH<sub>3</sub>, 3 H), 6.62-6.70 (m, ArH, 5 H), 7.66 (d, J = 8.6 Hz, ArH, 2 H), 9.66 (s, -CHO, 1 H).

**Compound 4:** Sodium hydride (0.36 g, 15 mmol) was added to a solution of compound 3 (2.7 g, 7.5 mmol) in 1,2-dimethoxyethane (5 ml). The solution was stirred for 5 min. and diethyl 4-(methylsulfonyl)benzyl phosphate (2.3 g, 7.5 mmol) was added dropwise. The red solution was stirred at 75°C for 10 hr. The solution was poured into crushed ice (50 g) under nitrogen. It was extracted with dichloromethane (3 X 20 ml). The combined organic solution was washed with water (30 ml) and brine (30 ml). After

removal of the solvent, the crude product was chromatographed in a silica gel column, using CH<sub>2</sub>Cl<sub>2</sub>/MeOH (100:1) as the eluent to give a bright yellow liquid (compound 4) (1.6 g, 63%). <sup>1</sup>H NMR (CDCl<sub>3</sub>, ppm): δ 1.34-1.58 (m, -C<sub>4</sub>H<sub>8</sub>-, 8 H), 2.56 (t, J = 7.5 Hz, Ar-CH<sub>2</sub>-, 2 H), 2.96 (s, -NCH<sub>3</sub>, 3 H), 3.04 (s, -SO<sub>2</sub>CH<sub>3</sub>, 3 H), 3.32 (t, J = 7.5 Hz, -NCH<sub>2</sub>-, 2 H), 3.73 (s, -OCH<sub>3</sub>, 3 H), 3.74 (s, -OCH<sub>3</sub>, 3 H), 6.62 -6.73 (m, ArH, 5 H), 6.85 (d, J = 16.2 Hz, -HC=, 1 H), 7.13 (d, J = 16.2 Hz, -HC=, 1 H), 7.36 -7.81 (m, ArH, 6 H).

**Compound 5:** Compound 4 (1.6 g, 3.2 mmol) in dichloromethane (10 ml) was added slowly to a BBr<sub>3</sub>/CH<sub>2</sub>Cl<sub>2</sub> solution (1.7M, 5.7 ml, 9.6 mmol) at -78 °C. After the completion of the addition, the solution was warmed up slowly to room temperature and stirred for 24 hr. The solution was added to an ice-water mixture with vigorous stirring. The organic layer was separated, washed with water (25 ml), and dried over magnesium sulfate. After removal of the solvent, the crude product was separated in a silica gel column, using hexane/ethyl acetate (1:2) as the eluent to give a viscous yellow liquid (compound 5) (1.2 g, 80%). <sup>1</sup>H NMR (CDCl<sub>3</sub>, ppm): δ 1.34-1.58 (m, -C<sub>4</sub>H<sub>8</sub>-, 8 H), 2.52 (t, J = 7.5 Hz, Ar-CH<sub>2</sub>-, 2 H), 2.92 (s, -NCH<sub>3</sub>, 3 H), 3.02 (s, -SO<sub>2</sub>CH<sub>3</sub>, 3 H), 3.28 (t, J = 7.5 Hz, -NCH<sub>2</sub>-, 2 H), , 5.39 (br, s, -OH, 1 H), 5.71(br, s, -OH, 1 H), 6.56-6.61 (m, ArH, 5 H), 6.82(d, J = 16.2 Hz, -HC=, 1 H), 7.10(d, J = 16.2 Hz, -HC=, 1 H), 7.34(d, J = 8.4 Hz, ArH, 2 H), 7.51(d, J = 8.1 Hz, ArH, 2 H), 7.78(d, J = 8.1 Hz, ArH, 2 H).

**Monomer A:** Trifluoromethanesulfonic anhydride (1.9 ml, 11.7 mmol) was added slowly to a solution of compound 5 (1.90 g, 3.9 mmol) in pyridine (15 ml) at -20°C. The solution was stirred at room temperature for 24 hr. The solution was poured into water (20 ml) and then extracted with dichloromethane (3 x 20 ml). The combined organic layer was washed with water (3 x 20 ml) and dried over magnesium sulfate. After removal of the solvent, the crude product was separated in a silica gel column, using hexane/ethyl acetate (2:1) as the eluent. The collected product was recrystallized again with methanol to

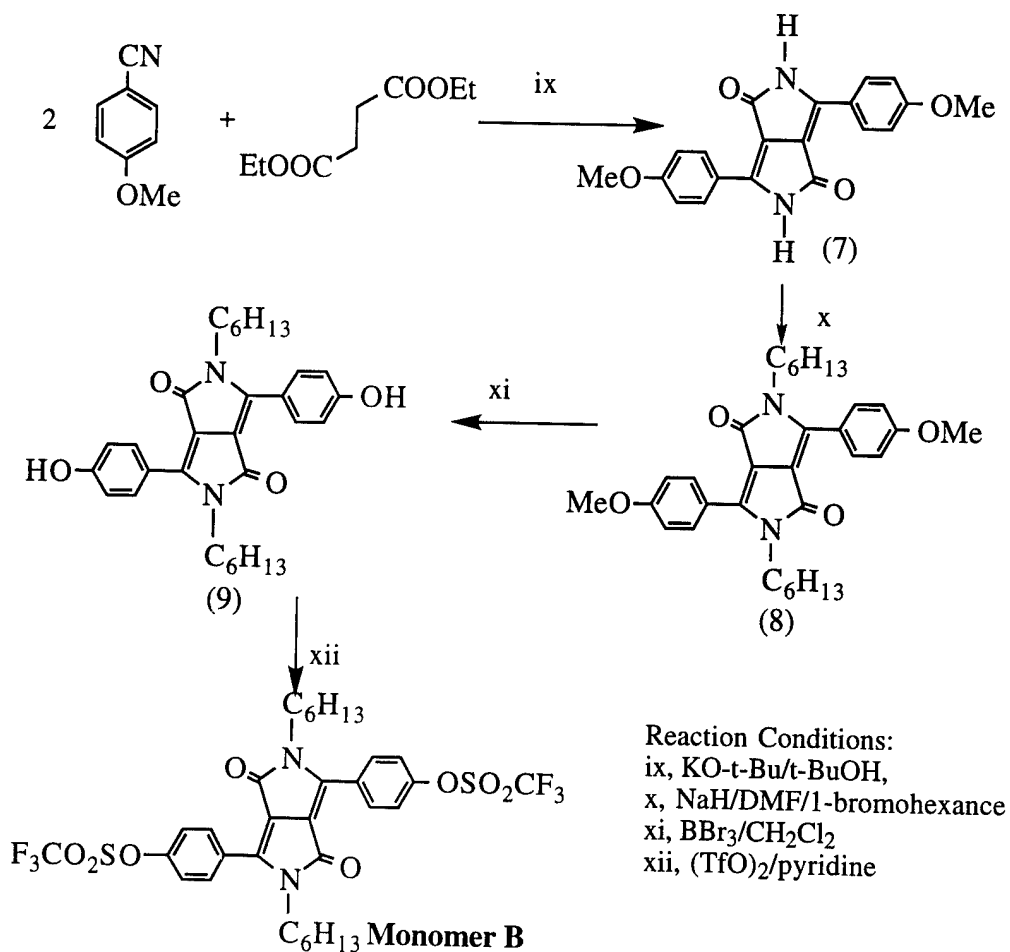
yield 1.30 g of a yellow solid (45%). mp, 94-96°C.  $^1\text{H}$  NMR ( $\text{CDCl}_3$ , ppm):  $\delta$ , 1.34-1.58 (m,  $-\text{C}_4\text{H}_8-$ , 8 H), 2.72 (t,  $J = 7.8$  Hz,  $\text{Ar}-\text{CH}_2-$ , 2 H), 2.96 (s,  $-\text{NCH}_3$ , 3 H), 3.04 (s,  $-\text{SO}_2\text{CH}_3$ , 3 H), 3.34 (t,  $J = 7.3$  Hz,  $-\text{NCH}_2-$ , 2 H), 6.63 (d,  $J = 8.0$  Hz,  $\text{ArH}$ , 2 H), 6.85 (d,  $J = 16.2$  Hz,  $-\text{HC}=\text{}$ , 1 H), 7.13 (d,  $J = 16.2$  Hz,  $-\text{HC}=\text{}$ , 1H), 7.16-7.31-7.81 (m,  $\text{ArH}$ , 9 H). Calcd for  $\text{C}_{30}\text{H}_{31}\text{NF}_6\text{O}_8\text{S}_3$ : C, 48.45; H, 4.20; N, 1.88. Found: C, 47.96; H, 4.08; N, 1.99.

**Compound 8:** Compound  $7^{18}$  (0.73 g, 2.1 mmol) and sodium hydride (0.13 g, 5.3 mmol) were added to DMF (8 ml). The solution was heated to reflux for 2 hr. It was then cooled down to room temperature and 1-bromohexane (0.88 g, 5.3 mmol) was added. The resulting mixture was heated under reflux for three additional hours. After being cooled to room temperature, the solution was filtered and the solid was washed with chloroform. The filtrate was then washed with water (3 x 20 ml). The organic solution was dried over anhydrous sodium sulfate. After removal of the solvent, the collected solid was recrystallized with methanol to afford compound 8 (0.20 g, 20%).  $^1\text{H}$  NMR ( $\text{CDCl}_3$ , ppm):  $\delta$  0.80 (t,  $J = 6$  Hz,  $\text{CH}_3-$ , 6 H), 1.20-1.65 (m,  $-(\text{CH}_2)_4-$ , 16 H), 3.75, (t,  $J = 7$  Hz,  $-\text{NCH}_2-$ , 4 H), 3.90 (s,  $-\text{OCH}_3$ , 6 H), 7.00 (d,  $J = 9$  Hz,  $\text{ArH}$ , 4 H), 7.8 (d,  $J = 9$  Hz,  $\text{ArH}$ , 4 H).

**Compound 9:** Boron tribromide (7.2 ml, 12 mmol) in  $\text{CH}_2\text{Cl}_2$  (10 ml) was added slowly to a solution of compound 8 (1.00 g, 2.0 mmol) in  $\text{CH}_2\text{Cl}_2$  (10 ml) at  $-78^\circ\text{C}$ . The solution was gradually warmed to room temperature and stirred for 24 hr. Water (10 ml) was slowly added to the solution. The resulting mixture was extracted with dichloromethane (3 x 20 ml). The combined organic layer was dried over magnesium sulfate and concentrated. The crude product was recrystallized with DMSO, yielding compound 9 as a red solid (0.79 g, 82%).  $^1\text{H}$  NMR ( $\text{DMSO}-d_6$ , ppm):  $\delta$  0.75 (t,  $J = 6.6$  Hz,  $\text{CH}_3-$ , 6 H), 1.10-1.40 (m,  $-(\text{CH}_2)_4-$ , 16 H), 3.66, (t,  $J = 7$  Hz,  $-\text{NCH}_2-$ , 4 H), 6.87 (d,  $J = 9$  Hz,  $\text{ArH}$ , 4 H), 7.66 (d,  $J = 9$  Hz,  $\text{ArH}$ , 4 H), 9.45 (br. s,  $-\text{OH}$ , 2H).

**Monomer B:** Trifluoromethanesulfonic anhydride (0.66 ml, 3.9 mmol) was added slowly to a solution of compound 9 (0.75 g, 1.56 mmol) in pyridine (5 ml) at 0°C. The resulting solution was stirred at room temperature for 24 hr. The color of the solution turned from red to light green during the course of the reaction. The solution was poured into water (10 ml). The solid was filtered, washed with water, and then recrystallized with a mixture of methanol and chloroform. Compound 10 was collected as yellow needle-shaped crystals (1.1 g, 94%, mp, 149-151°C). <sup>1</sup>H NMR (CDCl<sub>3</sub>, ppm): δ 0.80 (t, J = 6.6 Hz, -CH<sub>3</sub>, 6 H), 1.25-1.55 (m, -(CH<sub>2</sub>)<sub>4</sub>-, 16 H), 3.70 (t, J = 7 Hz, -NCH<sub>2</sub>-, 4 H), 7.40 (d, J = 9 Hz, ArH, 4 H), 7.90 (d, J = 9 Hz, ArH, 4 H). Calcd for C<sub>32</sub>H<sub>34</sub>N<sub>2</sub>F<sub>6</sub>O<sub>8</sub>S<sub>2</sub>: C, 51.06; H, 4.55; N, 3.72. Found: C, 50.76; H, 4.23; N, 3.76.

**Scheme 5:**



**Polymerization:** A typical polymerization procedure is exemplified by that for polymer I. To a 25 ml two-necked round bottom flask were added monomer A (0.296 g, 0.398 mmol), monomer B (0.210 g, 0.279 mmol), 2,5-bis(tributylstannyl)thiophene<sup>15</sup> monomer C, (0.448 g, 0.677 mmol), lithium chloride (86 mg, 2.0 mmol) and tetrakis(triphenyl-phosphine)palladium(0) (16 mg, 2 mol %) and 1,4-dioxane (4 ml). The mixture was heated at 90°C for 16 hr. The polymer was precipitated into methanol and was collected by filtration (almost quantitative yield). To further purify the polymer, it was dissolved in NMP and precipitated again into acetone. After being further washed with acetone in a Soxhlet extractor for 2 days, the polymer was collected as a dark red solid. The <sup>1</sup>H NMR data for polymers I to III are as follows (the numbering refers to Scheme 2): Polymer I:  $\delta$  (CD<sub>5</sub>Cl, ppm), 0.90 (b, H<sub>1</sub>), 1.25 (b, H<sub>2</sub>-H<sub>4</sub>), 1.40-1.80, (b, H<sub>5</sub>, H<sub>11</sub>-H<sub>14</sub>), 2.80, (s, H<sub>10</sub>), 2.90, (s, H<sub>16</sub>), 3.05, (s, H<sub>23</sub>), 3.30, (s, H<sub>15</sub>), 4.05, (b, H<sub>6</sub>), 6.4, (b, H<sub>17</sub>), 6.55, (d, J = 16.5 Hz, H<sub>19</sub>), 6.75 (d, J = 16.5 Hz, H<sub>20</sub>), 7.0-8.2 (b, heavily overlapped with solvent peaks, Aromatic).

Polymer II:  $\delta$  (CDCl<sub>3</sub>, ppm), 0.89 (b, H<sub>1</sub>), 1.30 (b, H<sub>2</sub>-H<sub>4</sub>), 1.40-1.70, (b, H<sub>5</sub>, H<sub>11</sub>-H<sub>14</sub>), 2.75, (t, J = 7.8 Hz, H<sub>10</sub>), 2.95, (s, H<sub>16</sub>), 3.05, (s, H<sub>23</sub>), 3.35, (t, J = 7.2 Hz, H<sub>15</sub>), 6.65, (d, J = 8.1 Hz, H<sub>17</sub>), 6.90, (d, J = 16.5 Hz, H<sub>19</sub>), 7.15 (d, J = 16.5 Hz, H<sub>20</sub>), 7.30 (m, H<sub>9</sub>), 7.40 (d, J = 8.1 Hz, H<sub>18</sub>), 7.52 (m, H<sub>7,8</sub>), 7.55 (d, J = 8.3 Hz, H<sub>21</sub>), 7.85 (d, J = 8.3 Hz, H<sub>22</sub>).

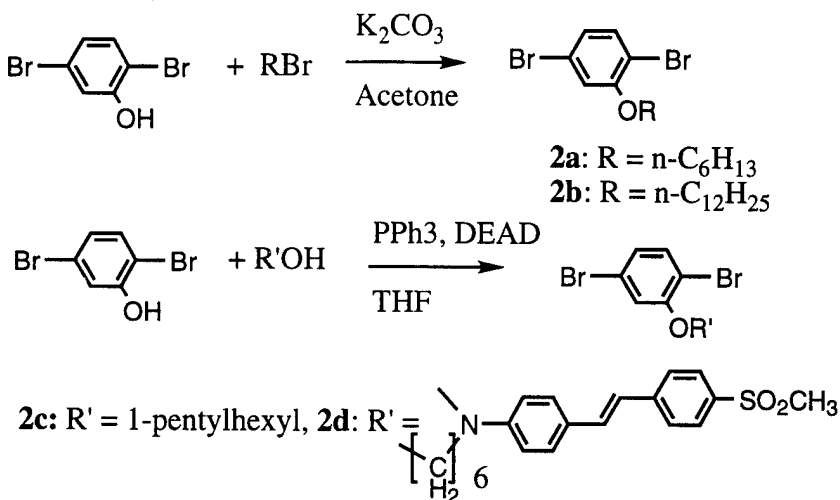
Polymer III:  $\delta$  (CDCl<sub>3</sub>, ppm), 1.40, 1.65, 1.70, (b, H<sub>11</sub>-H<sub>14</sub>), 2.75, (t, J = 7.8 Hz, H<sub>10</sub>), 2.95, (s, H<sub>16</sub>), 3.05, (s, H<sub>23</sub>), 3.35, (t, J = 7.2 Hz, H<sub>15</sub>), 6.65, (d, J = 8.1 Hz, H<sub>17</sub>), 6.90, (d, J = 16.5 Hz, H<sub>19</sub>), 7.15 (d, J = 16.5 Hz, H<sub>20</sub>), 7.30 (m, H<sub>9</sub>), 7.40 (d, J = 8.1 Hz, H<sub>18</sub>), 7.55 (d, J = 8.3 Hz, H<sub>21</sub>), 7.85 (d, J = 8.3 Hz, H<sub>22</sub>).

**General procedure for synthesizing 2,5-dibromoalkoxybenzenes:** 2,5-Dibromophenol (4.55 g, 18.1 mmol), alkyl bromide (18.1 mmol), potassium carbonate (2.5 g, 18.1 mmol), and acetone (50 ml) were added to a 100 ml two-necked, round-bottomed flask under a nitrogen atmosphere. The resulting mixture was refluxed for 24

hours and water (50 ml) was then added. The mixture was extracted with ether (3 × 50 ml). The combined organic layer was dried over anhydrous magnesium sulfate and then concentrated. The crude product was separated by silica gel chromatography using hexane as the eluent.

**2,5-dibromo-1-hexoxybenzene (2a):** Yield 89%.  $^1\text{H}$  NMR ( $\text{CDCl}_3$ , ppm)  $\delta$  7.32(d,  $J$  = 8.4 Hz, 1H), 6.95(d,  $J$  = 1.1 Hz, 1 H), 6.90(dd,  $J$  = 1.1, 8.4 Hz, 1 H), 3.97(t,  $J$  = 6.4 Hz, 2 H), 1.82(m, 2 H), 1.49(m, 2 H), 1.35(m, 4 H), 0.91(t,  $J$  = 6.6 Hz, 3 H).  $^{13}\text{C}$  NMR ( $\text{CDCl}_3$ )  $\delta$  156.3, 134.2, 124.6, 121.6, 116.6, 111.2, 69.6, 31.6, 29.1, 25.8, 22.8, 14.2. FTIR (neat) 2954, 2931, 2871, 2858, 1577, 1558, 1478, 1466, 1398, 1386, 1261, 1251, 1129, 1082, 1034, 1016, 944, 873, 837, 798  $\text{cm}^{-1}$ . Anal. Calcd. for  $\text{C}_{12}\text{H}_{16}\text{Br}_2\text{O}$ : C, 42.89; H, 4.80. Found: C, 42.94; H, 4.77.

**Scheme 6:**



**2,5-dibromo-1-dodecoxybenzene (2b):** Yield 78%. m.p. 31-32  $^{\circ}\text{C}$ .  $^1\text{H}$  NMR ( $\text{CDCl}_3$ , ppm)  $\delta$  7.32(d,  $J$  = 8.2 Hz, 1H), 6.94(d,  $J$  = 1.5 Hz, 1 H), 6.90(dd,  $J$  = 1.5, 8.2 Hz, 1 H), 3.97(t,  $J$  = 6.4 Hz, 2 H), 1.82(m, 2 H), 1.48(m, 2 H), 1.25-1.35(m, 16 H), 0.88(t,  $J$  = 6.2 Hz, 3 H).  $^{13}\text{C}$  NMR ( $\text{CDCl}_3$ )  $\delta$  156.3, 134.2, 124.6, 121.6, 116.5, 111.2, 69.6, 32.1, 29.9, 29.8, 29.6, 29.5, 29.1, 26.1, 22.9, 14.3. FTIR (neat) 2956, 2920, 2870, 2851, 1578, 1558, 1478, 1467, 1399, 1387, 1284, 1261, 1250, 1128,

1082, 1035, 1024, 1005, 870, 827, 801  $\text{cm}^{-1}$ . Anal. Calcd for  $\text{C}_{18}\text{H}_{28}\text{Br}_2\text{O}$ : C, 51.45; H, 6.72. Found: C, 51.57; H, 6.80.

**2,5-dibromo-1-(1-pentylhexoxy)benzene (2c):** 6-Undecanol (2.3 g, 13.1 mmol), 2,5-dibromophenol (3.0 g, 11.9 mmol), triphenylphosphine (4.7 g, 17.9 mmol), and THF (30 ml) were added to a 100 ml two-necked round-bottomed flask under a nitrogen atmosphere. The solution was cooled to 0 °C and diethylazodicarboxylate (DEAD) (2.3 ml, 14.3 mmol) was then added dropwise to the reaction mixture. The solution was stirred for 5 hours at room temperature. After removing the solvent with a rotary evaporator, the crude product was separated by silica gel chromatography using hexane as the eluent. The product was collected as a colorless liquid (4.8 g, 99 % yield).  $^1\text{H}$  NMR ( $\text{CDCl}_3$ , ppm)  $\delta$  7.31(d,  $J$  = 8.4 Hz, 1 H), 6.92(d,  $J$  = 1.6 Hz, 1 H), 6.87(dd,  $J$  = 1.6, 8.4 Hz, 1 H), 4.21(quin,  $J$  = 5.8 Hz, 1 H), 1.71-1.60(m, 4 H), 1.45-1.26(m, 12 H), 0.88(t,  $J$  = 6.8 Hz, 6 H).  $^{13}\text{C}$  NMR ( $\text{CDCl}_3$ )  $\delta$  156.0, 134.4, 124.5, 121.5, 118.0, 112.3, 80.4, 33.7, 32.0, 25.0, 22.8, 14.2. FTIR (neat) 2955, 2932, 2871, 2859, 1575, 1556, 1467, 1394, 1379, 1249, 1130, 1081, 1033, 997, 951, 877, 839, 796  $\text{cm}^{-1}$ . Anal. Calcd for  $\text{C}_{17}\text{H}_{26}\text{Br}_2\text{O}$ : C, 50.27; H, 6.45. Found: C, 50.41; H, 6.41.

**Compound 2d.** 4'-[(6-Hydroxyhexylmethylamino)-4-(methylsulfonyl)-stilbene]<sup>10</sup> (7.7 g, 19.8 mmol), 2,5-dibromophenol (5.0 g, 19.8 mmol), triphenylphosphine (7.8 g, 29.7 mmol), and THF (60 ml) were added to a 100 ml two-necked round-bottomed flask under a nitrogen atmosphere. The solution was cooled to 0°C and diethylazodicarboxylate (3.1 ml, 19.8 mmol) was added dropwise to the reaction mixture. The solution was stirred for 18 hours at room temperature. After removing the solvent with a rotary evaporator, the crude product was separated by a silica gel chromatography column using methylene chloride as the eluent. The product was then recrystallized with a chloroform/methanol mixture. The collected product was a yellow crystalline solid (9.5 g, 77% yield). m.p. 108-109°C.  $^1\text{H}$  NMR ( $\text{CDCl}_3$ , ppm)  $\delta$  7.81(d,  $J$  = 8.2 Hz, 2 H), 7.55(d,  $J$  = 8.2 Hz, 2 H), 7.36(d,  $J$  = 8.5 Hz, 2 H), 7.33(d,  $J$  = 8.3 Hz, 1 H), 7.13(d,  $J$  = 16.2 Hz, 1 H),



6.95(d,  $J = 1.2$  Hz, 1 H), 6.91(dd,  $J = 1.2, 8.3$  Hz, 1 H), 6.85(d,  $J = 16.2$  Hz, 1 H), 6.63(d,  $J = 8.5$  Hz, 2 H), 3.97(t,  $J = 6.2$  Hz, 2 H), 3.36(t,  $J = 7.2$  Hz, 2 H), 3.03(s, 3 H), 2.97(s, 3 H), 1.84(m, 2 H), 1.64(m, 2 H), 1.55(m, 2 H), 1.42(m, 2 H). FTIR (KBr) 2935, 2855, 1606, 1586, 1521, 1478, 1467, 1385, 1297, 1140, 1088, 1033, 965, 954, 869, 826, 802, 771  $\text{cm}^{-1}$ . Anal. Calcd for  $\text{C}_{28}\text{H}_{31}\text{Br}_2\text{NO}_3$ : C, 54.12; H, 5.03; N, 2.25. Found: C, 54.50; H, 4.77; N, 2.38.

**Polymerization:** A typical procedure for the synthesis of polymer **H** is described as follows: *p*-Divinylbenzene (0.132 g, 1.014 mmol), compound **2c** (0.412 g, 1.014 mmol), palladium(II) acetate (9.1 mg, 4 mol %), tri(*o*-methylphenyl)phosphine (62 mg, 0.2 equiv.), and DMF (5 ml) were added into a two-necked round-bottom flask under a nitrogen atmosphere. After a homogeneous solution was obtained, tributylamine (0.7 ml, 3 equiv.) was added to the solution. The reaction mixture was stirred at 100 °C for 24 hours and then poured into an excess amount of methanol (100 ml). The polymer was collected by filtration; it was redissolved in TCE and precipitated again into methanol. The collected orange-yellow solid was washed in a Soxhlet extractor with methanol for 2 days, and the final yield of the polymer was 71 %.

**Polymer Characterization.** The  $^1\text{H}$  NMR spectra were collected on a UC 500-MHz spectrometer. The  $^{13}\text{C}$  spectra were obtained using a GE QE 300-MHz spectrometer. The FTIR spectra were recorded on a Nicolet 20 SXB FTIR spectrometer. The UV-vis spectra were recorded on a Perkin-Elmer Lambda 6 UV/vis spectrophotometer. GPC measurements were performed using a Waters RI system equipped with a UV detector, a differential refractometer detector, and an Ultrastyrigel linear column at 35 °C using THF as the eluent. The molecular weights were calculated based upon monodispersed polystyrene standards. Thermal analyses were performed by using DSC-10 and TGA-50 systems from TA instruments under a nitrogen atmosphere with heating rates of 10 and 15 °C/min., respectively. The polarizing microscopic observation was performed with a

Nikon OPTIPHOT-2 microscope equipped with a Creative Devices 50-600 high temperature stage.

The photoconductivity was studied by measuring the voltage resulting from a photocurrent running through the sample and across a 1-M $\Omega$  resistor.<sup>11</sup> A He-Ne laser (632.8 nm) was used as the light source.

The second order NLO activities of corona poled polymer films were characterized by performing a second harmonic generation experiment. The poling conditions were as follow: temperature, 100 °C; voltage, 3 kV at the needle point; gap distance, 1 cm; poling current < 1  $\mu$ A. A mode-locked Nd:YAG laser (Continuum PY61C-10, 10-Hz repetition rate) was used as the light source. The second harmonic signal generated by the fundamental wave (1064 nm) was detected by a photomultiplier tube (PMT). After amplification it was averaged in a boxcar integrator. A quartz crystal was used as the reference sample.

An electro-optic coefficient ( $r_{33}$ ) was determined by the simple reflection technique.<sup>12</sup> A polymer film with a thickness of 2-3  $\mu$ m was prepared by casting a TCE solution of polymer onto an indium-tin oxide (ITO) glass. After corona poling, a silver electrode of 700 Å was deposited on the polymer film by vacuum evaporation. A He-Ne laser (632.8 nm) and a diode laser (780 nm) were used as the light sources.

Cyclic voltammetry (CV) was performed in an EG&G Princeton Applied Research Potentiostat interfaced to a personal computer. A thin polymer film was coated onto a Pt disc working electrode (diameter = 2 mm). The counter and reference electrodes were both Pt wire and the system was calibrated against the formal potential of [Cp<sub>2</sub>Fe]/[Cp<sub>2</sub>Fe<sup>+</sup>] couple (+0.40V vs. SCE). The experiment was carried out in acetonitrile (10 ml) with tetrabutylammonium tetraborofluorate (0.33 g) as a supporting electrolyte under a nitrogen atmosphere.

### **Functionalized Polyimides<sup>15,17</sup>**

The third type of PR polymers contain NLO chromophores and porphyrin-electron acceptor (quinones or imide) moieties. This PR system was designed based upon the fact that porphyrin-electron acceptor (quinones or imide moieties) systems are well known model compounds for photosynthetic processes and exhibit very interesting charge transfer properties.<sup>44</sup> A high quantum yield of charge separation can be achieved in these systems. Polyimides were found to be photoconductive and to allow charge transport.<sup>45</sup> Furthermore, polyimides possess high glass transition temperatures and therefore their electric field-induced dipole orientations can be fixed after imidization.

[illegible]

35

This polyimide was photoconductive and second order nonlinear-optically active. The photoconductivity of the polyimide was determined to be  $1.1 \times 10^{-12} \Omega^{-1} \text{cm}^{-1}$  under an external field of 1500 kV/cm using a diode laser ( $\lambda = 690 \text{ nm}$ ) as the light source ( $I = 5.9 \text{ mW/cm}^2$ ). After the sample was poled using a corona poling technique (poling field 2 mV/cm), second harmonic generation measurements revealed a sizable  $d_{33}$  value (ca. 110 pm/V at 1064 nm). This photorefractive polyimide exhibited very high temporal stability in dipole orientation at elevated temperatures. There was no significant decay in the  $d_{33}$  value at 90 °C and 150 °C. Long term stability was observed even at 170 °C, the initial  $d_{33}$  value of 80% was retained after 120 hours.

This polyimide demonstrated interesting photorefractive effects. For instance, an asymmetric optical energy exchange in the two beam coupling experiment has been observed. For an unpoled sample, no such phenomena were observed. A very large optical gain coefficient ( $22.2 \text{ cm}^{-1}$ ) under zero-field conditions was detected. This unusually large optical gain originated from the existence of an internal field in the poled polymer samples.

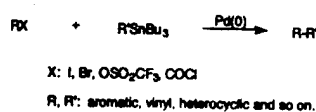
## ***Part II: Exploration of the Stille Coupling Reaction for the Synthesis of Functional Polymers***

To synthesize multifunctional polymers, a challenging task is to develop a novel synthetic approach so that many functional groups involved can survive. For this reason, we have devoted a great deal of research to explore the Stille coupling reaction for polycondensation because this reaction only requires mild conditions and can tolerate many functional groups. For example, the Stille coupling reaction enabled us to synthesize photorefractive polymers with conjugated backbones and pendant nonlinear optical chromophores. Approaches other than the palladium-catalyzed reactions will encounter problems of intolerance for many of these functional groups. To effectively utilize these

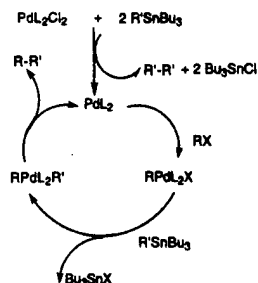
reactions for polycondensations, we have carried out detailed studies of the Stille reactions for polycondensations, including the reaction conditions and scopes .

The Stille reaction involves the coupling of an organic halide, triflate, or carbonyl chloride with organotin compound catalyzed by a palladium(0) catalyst. The organic groups can be aryl, heterocyclic or vinyl types. The reaction has been shown to tolerate many functional groups, such as amines, aldehydes, esters, ethers and nitro groups. The reaction yield is usually high which is essential to obtain high molecular weight polymers. A general reaction is shown in Scheme 8

**Scheme 8.** General Scheme for the Stille Coupling Reaction



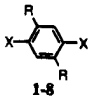
**Scheme 9.** Mechanism for the Stille Coupling Reaction



A proposed mechanism is shown in Scheme 9 which has been well accepted after a large amount of research by several groups. A palladium(II) or palladium(0) complex is generally introduced as the catalyst. When a palladium(II) compound is used, it is believed that it is first reduced to the palladium(0) species by the organotin compound. The resulting Pd(0) reacts with the organic halide or triflate to form the organopalladium halide (triflate) intermediate by oxidative addition. This intermediate then undergoes transmetalation. In the case of triflates, LiCl has to be used to facilitate this process.<sup>20</sup> Finally, a reductive elimination affords the product and the palladium(0) species to complete the catalytic cycle. Several review papers are available on the Stille coupling reaction, where various examples of the Stille reaction in organic synthesis are cited.

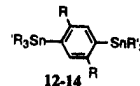
The general reaction conditions for the Stille reaction in the synthesis of small molecules have been studied. Nevertheless, studies on the reaction conditions for

polymerizations are limited. Many of the factors that may not affect the reactions for small molecules could drastically affect the molecular weight for polymerizations; examples are the monomer stoichiometric imbalance caused by the conversion of the palladium(II) catalyst to palladium(0), the solubility of the polymer in the reaction medium, the nature of the reactants, solvent, and the composition of the catalyst systems. To synthesize high molecular weight materials, it is of great importance to investigate these factors.



Compound	R	X
1	OC <sub>8</sub> H <sub>17</sub>	I
2	OC <sub>8</sub> H <sub>17</sub>	Br
3	OC <sub>8</sub> H <sub>17</sub>	OTf
4	C <sub>8</sub> H <sub>17</sub>	I
5	C <sub>8</sub> H <sub>17</sub>	Br
6	C <sub>8</sub> H <sub>17</sub>	OTf
7	OC <sub>11</sub> H <sub>23</sub>	OTf
8	no substitution	OTf

**Figure 8.** Structures of the organohalides and triflates for the Stille coupling reactions.



Compound	R	R'
12	OCH <sub>3</sub>	CH <sub>3</sub>
13	OCH <sub>3</sub>	<i>n</i> -C <sub>4</sub> H <sub>9</sub>
14	OC <sub>7</sub> H <sub>15</sub>	CH <sub>3</sub>

**Figure 9.** Structures of the organotin monomers for the Stille coupling reactions.

## Experimental Section

**2,5-Dioctanyl-1,4-bistriflate benzene (6).** To an ice cooled pyridine solution (8 mL) of 2,5-dioctanyl hydroquinone **16** (2.88 g, 8.6 mmol) was added triflate anhydride (3.05 mL, 18.1 mmol) dropwise. The reaction mixture was warmed to room temperature 30 minutes after the addition and stirred at room temperature for an additional 48 hours. This mixture was then poured into water (30 mL) and extracted with ether (20 mL, 2x). The organic layers were combined and washed consecutively with water (20 mL), 10% hydrochloric acid aqueous solution (10 mL, 2x), saturated sodium chloride aqueous solution (20 mL), and water (20 mL). The solution was dried over anhydrous magnesium sulfate and the solvent was evaporated under a vacuum. The crude product was purified by a short silica-gel column using hexane/ethyl acetate (40:1, v/v) as the eluent. Recrystallization from hexane gave a white solid; yield 95%. m.p. 30-30.5 °C. <sup>1</sup>H

NMR (CDCl<sub>3</sub>)  $\delta$  0.87 (t,  $J$  = 6.68 Hz, -CH<sub>3</sub>, 6H), 1.27 (m, -(CH<sub>2</sub>)<sub>5</sub>-, 20H), 1.58 (m, -CH<sub>2</sub>-, 4H), 2.65 (t,  $J$  = 7.83 Hz, Ar-CH<sub>2</sub>-, 4H), 7.14 ppm (s, phenyl protons, 2H). <sup>13</sup>C NMR (CDCl<sub>3</sub>)  $\delta$  14.03, 22.60, 29.11, 29.18 (2 carbons), 29.52, 29.63, 31.76, 118.12 (d,  $J$  = 320.29 Hz), 123.53, 135.42, 146.47 ppm. Anal. Calcd for C<sub>24</sub>H<sub>36</sub>O<sub>6</sub>S<sub>2</sub>F<sub>6</sub>: C, 48.15; H, 6.06. Found: C, 47.82; H, 6.00.

***p*-Bistriflate benzene (8).** This compound was synthesized in the same way as described for compound **6** from hydroquinone. Yield 75%. m.p. 50-52 °C. <sup>1</sup>H NMR (CDCl<sub>3</sub>)  $\delta$  7.35 ppm (s, phenyl protons, 4H). <sup>13</sup>C NMR (CDCl<sub>3</sub>)  $\delta$  118.12 (d,  $J$  = 320.18 Hz), 123.41, 148.41 ppm. Anal. Calcd for C<sub>8</sub>H<sub>4</sub>O<sub>6</sub>S<sub>2</sub>F<sub>6</sub>: C, 25.68; H, 1.08. Found: C, 25.69; H, 1.08.

**1,4-Bis(trimethyl stannyl) benzene (11).** The Grignard reagent of *p*-dibromobenzene was prepared by refluxing the mixture of *p*-dibromobenzene (6.60 g, 20 mmol) and magnesium powder (1.03 g, 42 mmol) in THF for two hours. To this solution cooled in an ice-bath was added a 2.5 M THF solution of trimethyltin chloride (16.4 mL, 41 mmol). The mixture was refluxed for 24 hours and then cooled in an ice-bath. After it was quenched with saturated ammonium chloride aqueous solution, the THF was evaporated under reduced pressure. The resulting suspension was extracted with ether (20mL, 3x). The combined organic layer was washed with water (20mL, 2x). It was then dried with anhydrous magnesium sulfate and the solvent was evaporated under reduced pressure to give a white solid. This solid was run through a silica-gel filtration column (hexane as the eluent) and recrystallized twice from methanol/ethyl acetate (20:1 v/v). Yield 30%. m.p. 117-120 °C. <sup>1</sup>H NMR (CDCl<sub>3</sub>):  $\delta$  0.27 (s, -Sn(CH<sub>3</sub>)<sub>3</sub>, 18H), 7.41 ppm (s, phenyl protons, 4H). <sup>13</sup>C NMR (CDCl<sub>3</sub>)  $\delta$  -9.39, 135.79, 142.41 ppm. Anal. Calcd for C<sub>12</sub>H<sub>22</sub>Sn<sub>2</sub>: C, 35.70; H, 5.50. Found: C, 35.67; H, 5.19.

**1,4-Bis(trimethyl stannyl)-2,5-dimethoxybenzene (12).** To a mixture of *p*-anisole (1.38 g, 10mmol) and tetramethylethylenediamine (4.53 mL, 30 mmol) in 40 mL of dry hexane was added a 2.5 M hexane solution of butyl lithium (15 mL, 37.5 mmol).



The mixture was stirred for 20 hours under room temperature. After stirring, the solution was cooled with an ice-bath and a 1.0 M hexane solution of trimethyltin chloride (43 mL, 43 mmol) was added dropwise. The mixture was then stirred under room temperature for 2 hours. After being quenched with water, the organic layer was separated and the aqueous layer was extracted with ether (20 mL, 2x). The organic layers were combined and washed with water. The solution was dried over anhydrous magnesium sulfate and the solvent was evaporated under reduced pressure. The resulting solid was purified chromatographically using a silica-gel column and hexane/ethyl acetate (40:1, v/v) as the eluent. The crude product was recrystallized from methanol to give 2.52 g of white solid (yield 54%). m.p. 114.5-115 °C.  $^1\text{H}$  NMR ( $\text{CDCl}_3$ )  $\delta$  0.26 (s,  $-\text{Sn}(\text{CH}_3)_3$ , 18H), 3.75 (s,  $-\text{OCH}_3$ , 6H), 6.82 ppm (s, phenyl protons, 2H).  $^{13}\text{C}$  NMR ( $\text{CDCl}_3$ )  $\delta$  -8.92, 56.36, 117.78, 132.28, 158.61 ppm. Anal. Calcd for  $\text{C}_{14}\text{H}_{26}\text{Sn}_2\text{O}_2$ : C, 36.26; H, 5.65. Found: C, 36.27; H, 5.82.

**1,4-Bis(tributyl stannyl)-2,5-dimethoxybenzene (13).** This compound was prepared in a similar method as for 1,4-bis(trimethyl stannyl)-2,5-dimethoxybenzene (**12**) except that tributyltin chloride was used instead of trimethyltin chloride. The resulting product was a colorless liquid. It was first vacuum distilled and then the component (1.3 Torr) was collected at 102-110 °C. Further purification was carried out by using a silica-gel column with hexane as the eluent. Yield 26%.  $^1\text{H}$  NMR ( $\text{CDCl}_3$ )  $\delta$  0.88 (t,  $J = 7.12$  Hz,  $-\text{CH}_3$ , 18H), 1.01 (m,  $-\text{CH}_2-$ , 12H), 1.32 (m,  $-\text{CH}_2-$ , 12H), 1.52 (m,  $-\text{SnCH}_2-$ , 12H), 3.71 (s,  $-\text{OCH}_3$ , 6H), 6.79 ppm (s, phenyl protons, 2H).  $^{13}\text{C}$  NMR ( $\text{CDCl}_3$ )  $\delta$  10.02, 13.85, 27.57, 29.41, 55.75, 117.22, 131.54, 158.41 ppm. Anal. Calcd for  $\text{C}_{32}\text{H}_{62}\text{Sn}_2\text{O}_2$ : C, 53.66; H, 8.73. Found: C, 53.68; H, 9.01.

**1,4-Bis(trimethyl stannyl)-2,5-diheptanoxybenzene (14).** This compound was prepared in a similar method as for 1,4-bis(trimethyl stannyl)-2,5-dimethoxybenzene **12** from *p*-diheptanoxybenzene. The resulting product was a white solid. Yield 35%. m.p. 74-76 °C.  $^1\text{H}$  NMR ( $\text{CDCl}_3$ )  $\delta$  0.26 (s,  $-\text{Sn}(\text{CH}_3)_3$ , 18H), 0.89

(t,  $J = 6.95$  Hz,  $-\text{CH}_3$ , 6H), 1.30 (m,  $-(\text{CH}_2)_3-$ , 12H), 1.45 (m,  $-\text{CH}_2-$ , 4H), 1.73 (m,  $-\text{CH}_2-$ , 4H), 3.87 (t,  $J = 6.95$  Hz,  $-\text{OCH}_2-$ , 4H), 6.79 ppm (s, phenyl protons, 2H).  $^{13}\text{C}$  NMR ( $\text{CDCl}_3$ )  $\delta$  -8.96, 14.11, 22.64, 26.13, 28.97, 29.13, 29.69, 31.84, 68.21, 117.11, 131.77, 157.54 ppm. Anal. Calcd for  $\text{C}_{26}\text{H}_{50}\text{Sn}_2\text{O}_2$ : C, 49.41; H, 7.97. Found: C, 49.66; H, 8.13.

**1,4-Dimethoxyl-2,5-dioctanylbenzene (15).** To a mixture of hydroquinone dimethyl ether (2.76 g, 20mmol) and tetramethylethylenediamine (9.1 mL, 60 mmol) in 40 mL dry hexane was added a 1.6 M hexane solution of butyl lithium (37.5 mL, 60 mmol). The mixture was stirred under room temperature for 20 hours. After the solution was cooled in an ice-bath, *n*-bromooctane (16 mL, 92 mmol) was added dropwise. The mixture was then stirred under room temperature for 12 hours. After being quenched with water, the organic layer was separated and the aqueous layer was extracted with ether (20 mL, 2x). The organic layers were combined and washed with water. The solution was dried over anhydrous magnesium sulfate and the solvent was evaporated under reduced pressure. The resulting liquid was vacuum distilled and the component was collected at 90-100 °C (0.3 Torr). It was then purified using a silica-gel column and hexane/chloroform (1:1, v/v) as the eluent. The crude product was recrystallized from methanol to give needle-like white crystals. Yield 48%. m.p. 50-51 °C.  $^1\text{H}$  NMR ( $\text{CDCl}_3$ )  $\delta$  0.87 (t,  $J = 6.26$  Hz,  $-\text{CH}_3$ , 6H), 1.29 (m,  $-(\text{CH}_2)_5-$ , 20H), 1.55 (m,  $-\text{CH}_2-$ , 4H), 2.54 (t,  $J = 7.79$  Hz, Ar- $\text{CH}_2-$ , 4H), 3.75 (s,  $-\text{OCH}_3$ , 6H), 6.60 ppm (s, phenyl protons, 2H).  $^{13}\text{C}$  NMR ( $\text{CDCl}_3$ )  $\delta$  14.14, 22.72, 29.36, 29.57, 29.71, 30.21, 30.28, 31.97, 56.18, 113.01, 129.25, 151.23 ppm.

**2,5-Dioctanyl hydroquinone (16).** To a methylene chloride solution (60mL) of 1,4-dimethoxy-2,5-dioctanylbenzene **15** (3.41 g, 9.4 mmol) cooled to -78 °C was added a solution of 3.6 M boron tribromide in methylene chloride (5.49 mL, 19.8 mmol). The solution was slowly warmed to room temperature and stirred for 12 hours. It was then quenched with water. Methylene chloride was evaporated under reduced pressure. The

white solid was filtered and rinsed with water. Recrystallization from hexane gave white flakes; Yield 92%. m.p. 102.5-103 °C.  $^1\text{H}$  NMR ( $\text{CDCl}_3$ ),  $\delta$  0.87 (t,  $J = 6.26$  Hz,  $-\text{CH}_3$ , 6H), 1.26 (m,  $-(\text{CH}_2)_5-$ , 20H), 1.56 (m,  $-\text{CH}_2-$ , 4H), 2.49 (t,  $J = 7.72$  Hz,  $\text{Ar}-\text{CH}_2-$ , 4H), 4.20 (s,  $-\text{OH}$ , 2H), 6.50 ppm (s, phenyl protons, 2H).

**Polymerization.** The typical polymerization procedures were as follows: For the polymerization of a diiodo monomer with a distannyl monomer, the two monomers (1 mmol each) were dissolved in 10 mL of dry THF and  $\text{PdCl}_2(\text{PPh}_3)_2$  (2 mol% equiv.) was added as the catalyst. The solution was refluxed under nitrogen until the black metallic palladium precipitated out. The mixture was filtered to remove the metallic palladium and the filtrate was then concentrated to about 10 mL and precipitated into acetone. The precipitate was collected by filtration, redissolved, and precipitated into acetone again. The polymer was collected and extracted with acetone for over 20 hours and then dried under a vacuum.

For the polymerization of ditriflate and distannyl monomers,  $\text{Pd}(\text{PPh}_3)_4$  (2 mol% equiv.) was used as the catalyst and 10 mL of dry 1,4-dioxane was added as the solvent. Lithium chloride (3 equiv.) was added and the solution was refluxed until the catalyst decomposed. The polymer was purified according to the same procedure described above.

**Poly(2,5-dialkylphenylene-1,4-thiophene) (polymer 1).**  $^1\text{H}$  NMR ( $\text{CDCl}_3$ ):  $\delta$  0.86-1.94 (broad peaks,  $-(\text{CH}_2)_n\text{CH}_3$ ), 2.88 (broad,  $-\text{phenyl}-\text{CH}_2-$ , 4H), 7.02 (broad, thiophenyl protons, 2H), 7.34 ppm (broad, phenyl protons, 2H).  $^{13}\text{C}$  NMR ( $\text{CDCl}_3$ , polymer 1,  $n = 6$ )  $\delta$  14.11, 22.62, 29.37, 31.60, 31.66, 33.31, 126.41, 132.21, 133.40, 138.59, 142.66 ppm. Anal. Calcd. for  $(\text{C}_{22}\text{H}_{30}\text{S})_m$  ( $n = 6$ ): C, 80.92; H, 9.26;. Found: C, 80.13; H, 9.23; I, not detectable (from the end group).

**Poly(2,5-dialkoxyphenylene-1,4-thiophene) (polymer 2).**  $^1\text{H}$  NMR ( $\text{CDCl}_3$ ):  $\delta$  0.86-1.94 (broad peaks,  $-(\text{CH}_2)_n\text{CH}_3$ ), 4.10 (broad,  $-\text{OCH}_2-$ , 4H), 7.25 (broad, thiophenyl protons, 2H), 7.53 ppm (broad, phenyl protons, 2H).  $^{13}\text{C}$  NMR ( $\text{CDCl}_3$ , polymer 2,  $n = 16$ )  $\delta$  14.22, 22.85, 26.31, 26.44, 29.55, 29.67, 29.90, 32.11,

69.86, 112.80, 124.08, 126.06, 139.46, 149.65 ppm. Anal. Calcd. for  $(C_{42}H_{70}O_2S)_m$  ( $n = 16$ ): C, 78.94; H, 11.04;. Found: C, 76.97; H, 11.46; I, 2.59 (from the end group).

**Polymer 9:** Yield, 45%.  $\delta$  ( $CDCl_3$ , ppm), 1.25-1.80 (b,  $H_2-H_5$ ,  $H_{11}-H_{14}$ ), 2.85, (b,  $H_{10}$ ), 2.90, (s,  $H_{16}$ ), 3.00, (s,  $H_{23}$ ), 3.30, (b,  $H_{15}$ ), 6.55, (b,  $H_{17}$ ), 6.80 (d,  $H_{19}$ ), 7.05 (b,  $H_{20}$ ), 7.40 (b,  $H_9$ ), 7.45-7.55 (b,  $H_{18}$ ,  $H_{21}$ ,  $H_{27}$ ), 7.75 ppm (b,  $H_{22}$ ); Anal. Calcd. for  $(C_{32.32}H_{33.43}N_{1.03}S_{1.99}Zn_{0.01}O_{1.98})_m$ : C, 72.91; H, 6.33; N, 2.71. Found: C, 70.20; H, 6.19; N, 2.56.

**Polymer 10:** Yield, 41%.  $\delta$  ( $CDCl_3$ , ppm), 0.90 (b,  $H_1$ ), 1.25-1.80 (b,  $H_2-H_5$ ,  $H_{11}-H_{14}$ ), 2.65, (s,  $H_{24}$ ), 2.85, (b,  $H_{10}$ ), 2.90, (s,  $H_{16}$ ), 3.00, (s,  $H_{23}$ ), 3.30, (b,  $H_{15}$ ), 3.95, (b,  $H_6$ ), 6.55, (b,  $H_{17}$ ), 6.80 (d,  $H_{19}$ ), 7.05 (b,  $H_{20}$ ), 7.40 (b,  $H_9$ ), 7.45-7.55 (b,  $H_{18}$ ,  $H_{21}$ ,  $H_{27}$ ), 7.75 ppm (b,  $H_{22}$ ). Anal. Calcd. for  $(C_{32.64}H_{33.86}N_{1.06}S_{1.98}Zn_{0.02}O_{1.96})_m$ : C, 72.98; H, 6.35; N, 2.76. Found: C, 71.42; H, 6.22; N, 2.70.

**Polymer 11:** Yield, 43%.  $\delta$  ( $CDCl_3$ , ppm), 0.90 (b,  $H_1$ ), 1.25-1.80 (b,  $H_2-H_5$ ,  $H_{11}-H_{14}$ ), 2.65, (s,  $H_{24}$ ), 2.85, (b,  $H_{10}$ ), 2.90, (s,  $H_{16}$ ), 3.00, (s,  $H_{23}$ ), 3.30, (b,  $H_{15}$ ), 3.95, (b,  $H_6$ ), 6.55, (b,  $H_{17}$ ), 6.80 (d,  $H_{19}$ ), 7.05 (b,  $H_{20}$ ), 7.40 (b,  $H_9$ ), 7.45-7.55 (b,  $H_{18}$ ,  $H_{21}$ ,  $H_{27}$ ), 7.75 (b,  $H_{22}$ ), 7.98-8.02 (b,  $H_7-H_8$ ), 10.15 (s,  $H_{25}$ );

**Polymer 12:** Yield, 41%.  $\delta$  ( $CDCl_3$ , ppm), 1.25-1.80 (b,  $H_2-H_5$ ,  $H_{11}-H_{14}$ ), 2.85, (b,  $H_{10}$ ), 2.90, (s,  $H_{16}$ ), 3.00, (s,  $H_{23}$ ), 3.30, (b,  $H_{15}$ ), 6.55, (b,  $H_{17}$ ), 6.80 (d,  $H_{19}$ ), 7.05 (b,  $H_{20}$ ), 7.40 (b,  $H_9$ ), 7.45-7.55 (b,  $H_{18}$ ,  $H_{21}$ ,  $H_{27}$ ), 7.75 ppm (b,  $H_{22}$ ). Anal. Calcd. for  $C_{32.32}H_{33.43}N_{1.03}S_{1.99}Cu_{0.01}O_{1.98}$ : C, 72.91; H, 6.33; N, 2.71. Found: C, 71.49; H, 6.16; N, 2.63.

**Polymer 13:** Yield, 85%.  $^1H$  NMR ( $CDCl_3$ ):  $\delta$  1.00 (b,  $H_{23}$ ), 1.30 (b,  $H_{22}$ ), 1.40 (b,  $H_9-H_{10}$ ), 1.55 (b,  $H_8$ ), 1.80 (b,  $H_7$ ), 2.67 (b,  $H_6$ ), 3.60 (b,  $H_{18}$ ), 4.31 (b,  $H_{11}$ ), 6.80-6.90 (b,  $H_5$ ,  $H_3-H_4$ ), 7.22 (b,  $H_{14}$ ), 7.39 (b,  $H_{12}$ ), 7.46 (b,  $H_{13}$ ), 7.49 (b,  $H_1-H_2$ ), 7.70-7.80 (b,  $H_{16}-H_{17}$ ), 8.02 ppm (b,  $H_{15}$ ). Anal. Calcd. for  $(C_{28.30}H_{25.55}N_{1.05}S_{1.00}O_{0.10})_m$ : C, 82.10; H, 6.22; N, 3.55. Found: C, ; H, ; N,

**Polymer 14:** Yield, 91%.  $^1\text{H}$  NMR ( $\text{CDCl}_3$ ) :  $\delta$  1.40 (b,  $\text{H}_9\text{-H}_{10}$ ), 1.55(b,  $\text{H}_8$ ), 1.80 (b,  $\text{H}_7$ ), 2.67 (b,  $\text{H}_6$ ), 4.31 (b,  $\text{H}_{11}$ ), 6.80-6.90 (b,  $\text{H}_5$ ,  $\text{H}_3\text{-H}_4$ ), 7.22 (b,  $\text{H}_{14}$ ), 7.39 (b,  $\text{H}_{12}$ ), 7.46 (b,  $\text{H}_{13}$ ), 7.49 (b,  $\text{H}_1\text{-H}_2$ ), 8.02 ppm (b,  $\text{H}_{15}$ ). Anal. Calcd. for  $\text{C}_{28}\text{H}_{25}\text{NS}$ : C, 82.52; H, 6.14; N, 3.20. Found: C, 79.80; H, 6.09; N, 3.28.

## Reaction Scope

**Catalyst amount.** According to the the proposed mechanism, if a  $\text{Pd(II)}$  compound was used as the catalyst, it has to be reduced to a  $\text{Pd(0)}$  species by the organotin compounds. It was found earlier in the Stille coupling reaction of aromatic acid chloride with trimethylstannylbenzene using  $\text{Pd(II)}$  as the catalyst that the catalytically active zero-valent palladium species was generated by the reduction of the divalent catalyst by trimethylstannylbenzene through the formation of biphenyl as shown in eq. 1. As a result, a part of the tin monomer was consumed leading to an imbalance in the monomer stoichiometry. However, in order to obtain high molecular weight polymers, the monomer stoichiometry should be carefully balanced. Therefore, the effect of the catalyst concentration on the polymerization was studied. A simple reaction system was chosen for this purpose (shown in eq. 2). The amount of the catalyst,  $\text{Pd(PPh}_3)_2\text{Cl}_2$ , was varied under conditions where either equivalent amounts of both monomers were used or the amount of monomer **9** was adjusted by compensating the amount that may be consumed by the  $\text{Pd(II)}$  in the catalytic cycle. The results are shown in Table 2.

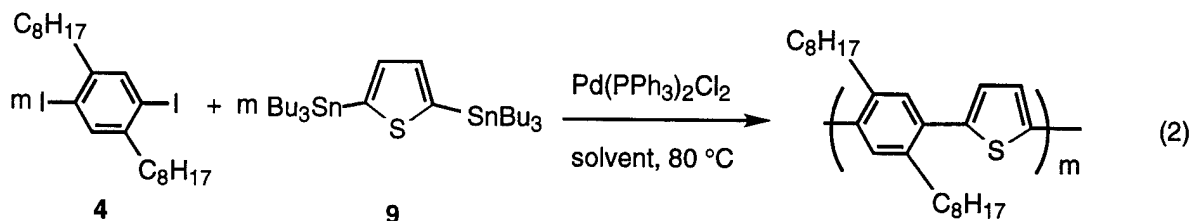
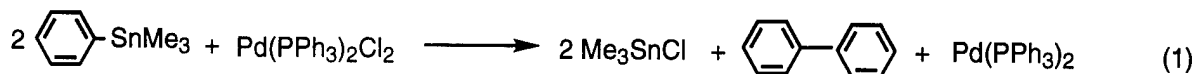


**Table 2.** Molecular Weights of Polymers from Eq 2<sup>a</sup>

entry	[Pd(II)] <sup>b</sup> (%)	$M_n(\text{C})$ <sup>c</sup>	DP(C) <sup>f</sup>	$M_n$ <sup>d</sup>	DP <sup>g</sup>
1	1	16 000 <sup>e</sup>	42	12 000	31
2	2	22 000	57	9 800	26
3	3	17 000	44	9 100	24
4	4	16 000	42	11 000	29
5	5	13 000	34	12 000	31

<sup>a</sup> Determined by GPC using polystyrenes as standards and THF as the eluent. <sup>b</sup> Mol % equiv of palladium catalyst (Pd(PPh<sub>3</sub>)<sub>2</sub>Cl<sub>2</sub>) (THF at 80 °C). <sup>c</sup>  $M_n(\text{C})$  is the number-averaged molecular weight obtained when the amount of monomer **2** was adjusted according to the amount of palladium catalyst used. For example, if 2 mol % equiv of Pd(II) was adapted, 1.02 equiv of monomer **2** would be used. <sup>d</sup>  $M_n$  is the number-averaged molecular weight using equivalent amounts of monomers. <sup>e</sup> Polymer partially soluble in THF. <sup>f</sup> DP(C) is the degree of polymerization obtained when the amount of monomer **2** was adjusted according to the amount of palladium catalyst used. <sup>g</sup> DP is the degree of polymerization using equivalent amounts of monomers.

It can be seen that the molecular weights obtained with corrections in monomer **9** are higher than those without corrections regardless of the amount of catalyst used. It should be pointed out that the molecular weight is determined by using polystyrenes as the standard samples which clearly can not give rise to the absolute molecular weight. However, the results should still be meaningful since the same polymer structure is compared. Thus, in these two cases, the effect of the catalyst concentration is different. For the reactions where the monomer amount was adjusted, the higher the catalyst concentration, the lower the molecular weight of the resulting polymer. When both monomers were used in equivalent amounts, the molecular weight first decreased when the catalyst concentration increased from 1 mol% equiv. to 3 mol% equiv. and then increased

when the catalyst concentration increased from 4 mol% equiv. and 5 mol% equiv. If all the initially active catalyst palladium(0) was formed as described in eq. 1, the higher the catalyst concentration the lower the molecular weight should be. When the monomer stoichiometry is adjusted, the molecular weight should not be greatly affected by the catalyst concentration. Our results indicate that the tin monomer is indeed responsible for the initial reduction of the palladium(II) catalyst since the adjustment of the monomer amount does improve the molecular weights. However, the exact amount of tin monomer that is consumed is not exactly clear and this amount may also depend on the concentration of the catalyst initially used. However, from the above results, the best reaction condition was identified and used in our further studies involving diiodo-monomers: catalyst,  $\text{Pd(PPh}_3)_2\text{Cl}_2$  (2 mol% equiv.) and the amount of tin monomer, 1.02 equivalent of the diiodo monomer.

**Solvent effect.** The solvent is known to play an important role in the Stille reaction.<sup>20,25</sup> In the polymerization process, solvent affects both the catalyst stability and the molecular weights of the resulting polymers. The ideal solvent for the palladium-catalyzed polymerization should be able to maintain the polymeric molecules in solution and at the same time stabilize the catalyst. Studies on several solvents commonly used in the Stille coupling reaction (eq. 2) showed that the highest molecular weight of the polymer was obtained when THF was used as the solvent (Table 3). This is due to the good solubility of the resulting polymers and the good stability of the Pd catalyst in THF solution. No precipitation of the catalyst was observed until reacting for seven days. The reactions proceeded to completion quickly in DMF and NMP which are known to accelerate the palladium-catalyzed reactions by acting as ligands to the palladium center.<sup>25</sup> However, the solubility of the resulting polymers was very limited in NMP and moderate in DMF. They precipitated out from the reaction medium and therefore their molecular weights were limited. The polymerization in dioxane was slow and the Pd catalyst was not as stable in this solvent as in THF and precipitated as the palladium black from the solution after two

days. The molecular weight was much lower than that obtained from the THF medium. Overall, we find that THF is a good solvent for the Stille coupling reaction. DMF would also be a good solvent if the desired polymer possesses a high solubility in it.

**Table 3.** Molecular Weights for Polymerization of 2,5-Dioctyl-1,4-diiodobenzene with 1,4-Bis(tributylstannanyl)thiophene Catalyzed by  $\text{Pd}(\text{PPh}_3)_2\text{Cl}_2$  (2 mol % equiv) in Different Solvents at 80 °C

solvent	$M_n^a$	$M_w^b$	polydispersity	DP <sup>c</sup>
dioxane	14 300	31 400	2.19	37
DMF	18 700	47 500	2.54	49
NMP	5 300	10 900	2.06	14
THF	21 700	60 200	2.77	57

<sup>a</sup> Number-averaged molecular weight. <sup>b</sup> Weight-averaged molecular weight. <sup>c</sup> Degree of polymerization.

**Ligand effect.** The polymerization of 2,5-dioctyl-1,4-diiodobenzene with 1,4-bis(tributylstannyl)-thiophene (eq. 2) was studied in the presence of different ligands. Here the tris(dibenzylideneacetone)dipalladium ( $\text{Pd}_2\text{dba}_3$ ) was used as the catalyst. When the reaction was carried out with a stoichiometric amount of the two monomers and 1 mol% equivalent of  $\text{Pd}_2\text{dba}_3$  (2 mol% equiv. of Pd), palladium black precipitated out from the solution when the mixture was heated to 80 °C. No reaction was observed and only the monomers were recovered. When different ligands were added, the effective catalyst  $\text{PdL}_4$  was formed *in situ* by ligand exchange between the weakly coordinated  $\text{Pd}_2\text{dba}_3$  and the ligand (4 equiv. for each Pd) under study. The purple red color of the  $\text{Pd}_2\text{dba}_3$  usually turned into a pale yellow color within 5-10 minutes at room temperature.

When  $\text{AsPh}_3$  was used as the ligand, the reaction was found to complete quickly, resulting in the polymer with the highest molecular weight (Table 3 entry 6). When tri-2-furylphosphine was used as the ligand, the reaction mixture became very viscous after 24 hours, but the palladium catalyst didn't decompose until after 7 days (Table 3 entry 9). The molecular weight obtained under this condition was relatively high. If triphenylphosphine



was used, the solution became viscous only after 3-4 days under the same conditions (Table 3 entry 3). Thus, the polymerization was faster with tri-2-furylphosphine as the ligand than with triphenylphosphine. If (2-MeC<sub>6</sub>H<sub>4</sub>)<sub>3</sub>P or P(OPh)<sub>3</sub> was used, the catalyst appeared to be unstable (Table 3 entry 7 and 8) and decomposed before high molecular weights of the polymers were formed.

**Table 4.** Molecular Weights for Polymerization of 2,5-Dioctyl-1,4-diiodobenzene with 1,4-Bis(tributylstannanyl)thiophene Catalyzed by Pd<sub>2</sub>dba<sub>3</sub> (1 mol %) in the Presence of Ligands at 80 °C in THF

entry	ligand (L)	Pd:L	<i>M</i> <sub>n</sub> <sup>a</sup>	<i>M</i> <sub>w</sub> <sup>b</sup>	DP <sup>d</sup>	polydispersity	reaction time <sup>c</sup>
1	PPh <sub>3</sub>	1:1	8 500	18 000	22	2.10	4.5 days
2		1:2	13 000	28 000	34	2.17	7 days
3		1:4	13 000	24 000	34	1.83	7 days
4	AsPh <sub>3</sub>	1:1	13 000	33 000	34	2.49	12 h
5		1:2	18 000	46 000	47	2.55	24 h
6		1:4	22 000	56 000	57	2.50	24 h
7	(2-MeC <sub>6</sub> H <sub>4</sub> ) <sub>3</sub> P	1:4	9 000	21 000	23	2.27	24 h
8	P(OPh) <sub>3</sub>	1:4	7 200	13 000	19	1.79	24 h
9	(2-fury) <sub>3</sub> P	1:4	18 000	40 000	47	2.23	7 days

<sup>a</sup> Number-averaged molecular weight. <sup>b</sup> Weight-averaged molecular weight. <sup>c</sup> The time for the palladium catalyst to decompose and precipitate out from the solution, after which the reaction was stopped.

<sup>d</sup> Degree of polymerization.

Catalysts with unsaturated coordination were examined by treating Pd<sub>2</sub>dba<sub>3</sub> with 1 or 2 equiv. of ligand (for each Pd) *in situ*. If only 1 equiv. of ligand was used, the resulting catalyst was unstable and decomposed before the reaction went to completion (Table 4 entry 1 and 4). Low molecular weight oligomers were formed. If 2 equivalents of ligand were used, the catalysts formed were much more stable (Table 4 entry 2 and 5) and the molecular weights were significantly higher than the former situation. When the ligand amount was increased to 4 equivalents, higher molecular weight was obtained if AsPh<sub>3</sub> was used and no difference was observed in molecular weight between two and four equivalents of PPh<sub>3</sub>. Therefore, to insure the highest molecular weight, 4 equivalents of ligand should be used in polymerization. From these results, the reactivity of the ligand

can be ranked as  $\text{AsPh}_3 > (2\text{-furyl})_3\text{P} > \text{PPh}_3$  which has a similar trend for other examples of the Stille coupling reactions.

Recently, some modified conditions for the Stille coupling reaction have been reported, such as using phosphine-free palladium sources to minimize the aryl-phenyl scrambling or by using  $\text{Pd(0)/Cu(I)}$  co-catalyst to accelerate the transmetallation.<sup>26-29</sup> When  $\text{Cu(I)}$  salt is applied, it reacts with organostannanes to produce transient organocopper intermediates which are presumably more reactive than organostannanes in transmetallation with the palladium species. We studied the effect of the addition of copper iodide (same condition as Table 3 entry 3 except 20% equiv. of  $\text{CuI}$  is added). Compared with the same reaction condition without copper iodide (Table 4 entry 3), the addition of  $\text{CuI}$  did not have a positive effect on the molecular weight. A weight averaged molecular weight of 11K Dalton with a polydispersity of 1.65 was obtained. This might be due to the limited solubility of copper iodide in the reaction medium THF. In a DMF or NMP medium, the effect of copper iodide can not be observed because our polymer precipitates out from these solvents before a higher molecular weight was reached.

**Reactivity of Different Monomers.** In order to expand the scope of the Stille coupling reaction to different conjugated polymer systems, we studied the reactivities of various monomers (Table 5). In general, diiodo-substituted monomers are more reactive than the dibromo-substituted. In the case of PPT and PPV, diiodo-monomers lead to higher molecular weights than dibromo-monomers (Table 5 entry 1, 4, 7, and 10). The dialkyl-substituted monomers gave higher molecular weights than the similar dialkoxy-substituted. However, very low reactivity was found for these monomers in preparing PPP type of polymers (Table 5 entry 13 and 15). The reaction could not proceed further after forming dimers or trimers. Two factors might be responsible for this difference. Firstly, the oxidative addition step in a palladium-catalyzed reaction is usually facilitated by electron-withdrawing or less electron-donating groups. Secondly, the dialkyl-substituted polymers have better solubility than the similar dialkoxy-substituted polymers. The triflate

monomers were reacted under different conditions from the dihalides. Low molecular weight polymers were obtained from DMF due to the low solubility of the polymer. Low molecular weights were also obtained when THF was used as the solvent because the reaction temperature could not be increased above 80 °C under ambient pressure.

**Table 5.** Preparations of Different Conjugated Polymers from the Reaction of Monomer **A** and Monomer **B** under the Stille Coupling Conditions

entry	monomer A	monomer B	$M_n^a$	$M_w^b$	DP <sup>c</sup>	polydispersity
1	9	1	4 300	8 300	10	1.96
2	9	2	2 100	4 300	5	2.04
3	9	3	5 600	9 100	14	1.61
4	9	4	12 400	29 600	32	2.39
5	9	5	9 500	26 700	25	2.81
6	9	6	8 300	11 200	22	1.36
7	10	1	2 600	5 100	7	1.92
8	10	2	1 800	2 100	5	1.15
9	10	3	3 200	4 800	9	1.48
10	10	4	4 200	11 500	13	2.75
11	10	5	1 900	6 900	6	3.72
12	10	6	3 900	8 000	12	2.05
13	11	1	no reaction			
14	11	3	4 900	9 100	12	1.88
15	11	4	no reaction			
16	11	6	4 300	5 200	11	1.22

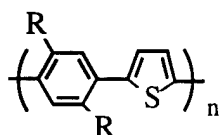
<sup>a</sup> Number-averaged molecular weight. <sup>b</sup> Weight-averaged molecular weight. <sup>c</sup> Degree of polymerization.

The reactivities of the three tin monomers **9**, **10**, and **11** were very different. The thiophenyl monomer **9** was the most reactive. High molecular weight polymers could be obtained (Table 5 entry 1-6). The electron-donating property of the sulfur atom may accelerate the transmetalation step which is generally accepted as the rate-determining step for palladium-catalyzed cross-coupling reactions.<sup>30,31</sup> The distannyl-substituted ethylene appeared to be much less reactive. Under the same conditions, only low molecular weight oligomers were obtained (Table 5 entry 7-12). Stannylbenzenes were usually found to be not very active under the Stille coupling conditions. We tested several types of stannylbenzenes, none of the substituted ones gave polymers. Only dimers or trimers were obtained (reactions of compound **12** and **6**, compound **13** and **6**, compound **14** and **8**). When a more hindered triflate monomer such as 2,5-di(*t*-butyl)-*p*-bis(trifluoromethyl)-sulfonylbenzene was used, no reaction occurred and the starting monomers were

recovered. These results indicated that both the oxidative addition and the transmetallation steps in the Stille reaction are sensitive to the steric bulkiness of the substituent on the reactants. Furthermore, the molecular weight was also increased by polymerizing monomer **7** with *p*-(bistributylstannyl)benzene instead of *p*-(bistrimethylstannyl)benzene **11**.<sup>32</sup> This might be due to a slower alkyl-transfer than aryl-transfer when the alkyl group is butyl.<sup>20</sup>

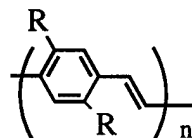
## Polymer Characterizations

**Structural Characterizations.** The polymers synthesized above have been characterized by different techniques, the results of which are partially discussed in this section to provide supports for the claimed polycondensations.



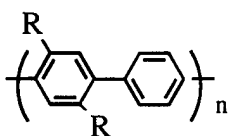
polymer **1** R:  $C_nH_{2n+1}$   
polymer **2** R:  $OC_nH_{2n+1}$

PPT



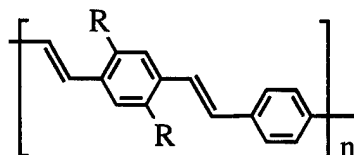
polymer **3** R:  $C_nH_{2n+1}$   
polymer **4** R:  $OC_nH_{2n+1}$

PPV



polymer **5** R:  $C_nH_{2n+1}$   
polymer **6** R:  $OC_nH_{2n+1}$

PPP



polymer **7** R:  $C_nH_{2n+1}$   
polymer **8** R:  $OC_nH_{2n+1}$

PPV

Since the final polymers are soluble in common organic solvents, such as THF, chloroform, toluene and dichloroethane, many physical characterizations can be performed.

The  $^1H$  NMR spectra of all polymers exhibit the chemical shifts of alkyl side-chains at 0.90-1.95 ppm. The methylene protons next to the oxygen atom ( $-O-CH_2-$ ) appears at

4.20 ppm, and the methylene protons adjacent to the phenyl rings are found at 2.88 ppm. In polymer 1, the chemical shifts of the thiophenyl proton and the phenyl proton appear at 7.02 and 7.34 ppm respectively, while they are found at 7.25 and 7.53 ppm in polymer 2. The vinyl protons of polymers 3 and 4 are at 7.20 and 7.11 ppm respectively. The protons on the phenyl ring are found at 7.37 ppm for polymer 3, and at 7.44 ppm for polymer 4. The chemical shift of the substituted phenyl ring protons appears at 7.17 ppm for polymer 5 and at 7.06 ppm for polymer 6. The unsubstituted phenyl ring protons are found at 7.40 and 7.66 ppm for polymers 5 and 6.

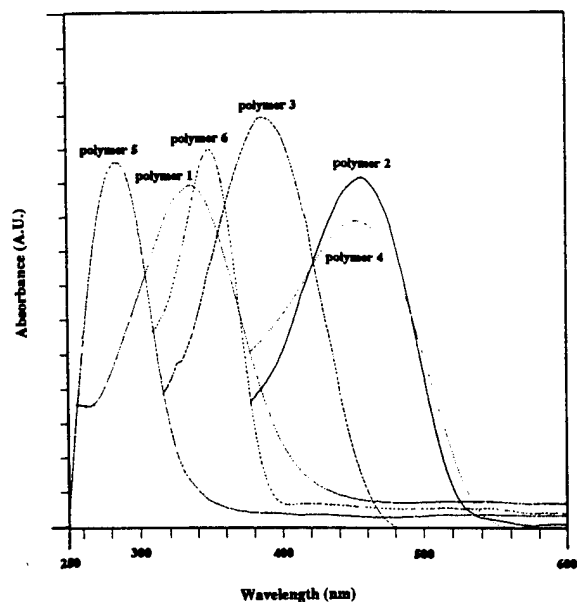


**Figure 10.** UV-vis spectra of different polymers measured in THF solutions.

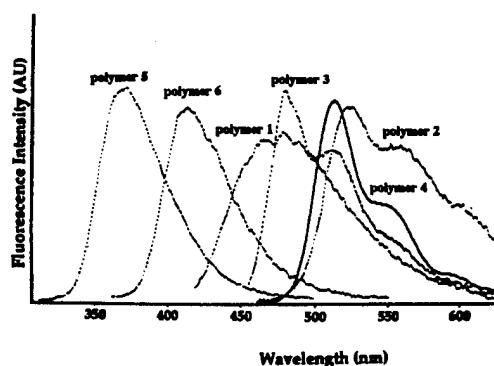


**Figure 5.** Photoluminescence spectra of different polymers measured in THF solutions.

The UV-vis/fluorescence spectra of several polymers are shown in Figures 10 and 11. The absorptions of the alkoxy-substituted polymers were red-shifted compared to the corresponding alky-substituted polymers due to the electronic effect and less steric hindrance. With the same substitution (either dialkyl or dialkoxy), PPP type of polymers absorbed at the highest energy region while PPTs absorbed at the lowest energy region. Similar trends were observed in the emission spectra of these polymers. It is interesting to observe that the emission spectra of these polymers prepared from the Stille coupling

reaction cover almost the entire visible spectral region. It is known that conjugated polymers with similar backbones are electroluminescent materials.<sup>34,35</sup> Polymers emitting different wavelengths of light can be used for full-color display.

**Thermal properties.** Table 6 summarizes the thermal transitions of different polymers. The melting temperatures determined by differential scanning calorimeter (DSC) were consistent with the polarizing microscopic observations. All the polymers were found to be liquid crystalline materials under the polarizing microscope. We previously demonstrated the liquid crystallinities of dialkoxy-substituted PPTs (polymer 2), PPPs (polymer 6) and PPVs (polymer 7 and 8). The dialkyl-substituted polymers are also liquid crystalline polymers. The PPVs prepared from the Heck reactions (polymer 7 and polymer 8) are structurally different from those prepared by the Stille coupling reactions (polymers 3 and polymer 4). However, both polymers 3 and 4 were found to be liquid crystalline polymers which may be due to their small molecular weights while similar polymers prepared from other approaches did not show LC properties.

**Table 6.** Thermal Transitions of Different Polymers

polymer	$T_g^a$ (°C)	$T_m^b$ (°C)	$T_c^c$ (°C)
1 <sup>d</sup>	55	98	100
2 <sup>d</sup>	47	120	148
3 <sup>d</sup>	30	75	135
4 <sup>e</sup>	50	67	160
5 <sup>d</sup>	34	58	120
6 <sup>f</sup>	80	155	242

<sup>a</sup> Glass transition temperature, determined by DSC. <sup>b</sup> Melting temperature, determined by DSC. <sup>c</sup> Clearing temperature, corresponding to the transition from the liquid crystalline state to the isotropic state, determined by a polarizing microscope. <sup>d</sup> The polymers were used as precipitated without any thermal treatment. <sup>e</sup> This polymer was annealed at 60 °C for 2 h. <sup>f</sup> This polymer was annealed at 50 °C for 2 h.

**Cyclic voltammetry.** To examine the electroactivities of these conjugated polymers, we performed cyclic voltammetry measurements. All the dialkoxy-substituted polymer films were oxidized irreversibly (Figure 12). A large electric current was noticed and the color of the film changed to black after one cycle. The current dropped dramatically

after each scan. Changing the scan rate shifted the peak value for oxidation. This oxidation is most likely due to the oxidation of the conjugated backbone. Similar phenomena have also been reported for alkoxy-substituted PPVs prepared by the Heck reaction.<sup>38</sup> Except PPTs, the dialkyl-substituted polymers could not be oxidized when they were scanned from 0.0 V to 2.2 V under different scan rates ranging from 20 mV/s to 1000 mV/s. This could be due to their lower HOMO orbital levels compared to dialkoxy-substituted polymers. The oxidation of the dialkyl PPT was also irreversible, resulting in a black substance. No reduction of the above polymer films from 0 to -3 V was observed at different scan rates.

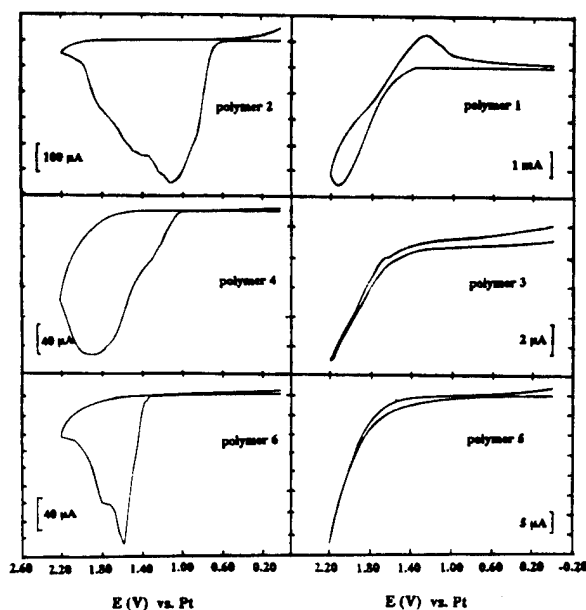


**Figure 2.** Cyclic voltammograms of different conjugated polymers (scan rate 200 mV/s).

### Concluding Remarks:

Synthesis and studies on the photorefractive effects of multifunctional polymers are a new research area which is filled with surprises and challenges. The past five years have witnessed a rapid growth in this area, especially, in composite polymer systems. Some of the characteristic parameters in these systems, such as optical gain, diffraction efficiency, have reached extraordinarily high values. However, the challenges we are facing are also

overwhelming: very little understanding has been gained on the mechanism for these photorefractive materials. Photoconductive polymers have been studied for many decades, their mechanism for photoconduction is still not well understood. In a photorefractive polymer, the introduction of electro-optic species makes the system tremendously more complicated. Further complications in composite systems arise from the fact that they suffer from phase separation and low glass transition temperatures. The approach to the fully functionalized PR polymers will clearly solve many of these problems. The work pursued in the past three years allowed us to develop novel synthetic approaches and demonstrated new design principles for PR polymers. Our most recent results showed great improvement in the PR performances by incorporating transition metal complexes into conjugated polymer backbones. Large net optical gains were obtained. Further research along this line will be pursued under continuous support from AFOSR.